Wetting phenomena in membrane distillation: Mechanisms, reversal, and prevention

Mohammad Rezaei [a,*], *David M. Warsinger* [b,c], *John H. Lienhard V* [c], *Mikel C. Duke* [d], *Takeshi Matsuura* [e], *Wolfgang M. Samhaber* [a]

[a] Institute of Process Engineering, Johannes Kepler University Linz, Altenberger Strasse 69, 4040 Linz, Austria

[b] Department of Chemical and Environmental Engineering, Yale University, New Haven, Connecticut 06520-8286, the USA

[c] Rohsenow Kendall Heat Transfer Laboratory, Department of Mechanical Engineering, Massachusetts Institute of Technology, 77 Massachusetts Avenue, Cambridge MA 02139-4307, USA

[d] Institute for Sustainability and Innovation, College of Engineering and Science, Victoria University, Melbourne, Victoria 8001, Australia

[e] Department of Chemical and Biological Engineering, University of Ottawa, Ottawa, Ontario K1N 6N5, Canada

*Corresponding Author: Tel: +4373224689747, Email: mohammad.rezaei@jku.at

M. Rezaei, D.M. Warsinger, J.H. Lienhard V, M. Duke, W.M. Samhaber, "Wetting phenomena in membrane distillation: mechanisms, reversal and prevention," *Water Research*, Vol. 139, pp. 329–352, 1 August 2018.

Abstract

Membrane distillation (MD) is a rapidly emerging water treatment technology; however, membrane pore wetting is a primary barrier to widespread industrial use of MD. The primary causes of membrane wetting are exceedance of liquid entry pressure and membrane fouling. Developments in membrane design and the use of pretreatment have provided significant advancement toward wetting prevention in membrane distillation, but further progress is needed. In this study, a broad review is carried out on wetting incidence in membrane distillation processes. Based on this perspective, the study describes the wetting mechanisms, wetting causes, and wetting detection methods, as well as hydrophobicity measurements of MD membranes. This review discusses current understanding and areas for future investigation on the influence of operating conditions, MD configuration, and membrane non-wettability characteristics on wetting phenomena. Additionally, the review highlights mathematical wetting models and several approaches to wetting control, such as membrane fabrication and modification, as well as techniques for membrane restoration in MD. The literature shows that inorganic scaling and organic fouling are the main causes of membrane wetting. The regeneration of wetting MD membranes is found to be challenging and the obtained results are usually not favorable. Several pretreatment processes are found to inhibit membrane wetting by removing the wetting agents from the feed solution. Various advanced membrane designs are considered to bring membrane surface non-wettability to the states of superhydrophobicity and superomniphobicity; however, these methods commonly demand complex fabrication processes or high-specialized equipment. Recharging air in the feed to maintain protective air layers on the membrane surface has proven to be very effective to prevent wetting, but such techniques are immature and in need of significant research on design,

Keywords: Membrane distillation; Membrane wetting; Hydrophobicity; Pretreatment; Membrane modification; Review

Contents

1. Introduction 4
2. Parameters for wetting 6
2.1. Liquid entry pressure 6
2.2. Membrane surface free energy 9
2.3. Surface wettability 10
3. Wetting mechanisms 11
4. Wetting detection 13
5. Causes of wetting 14
5.1. Inorganic fouling 16
5.2. Organic fouling 17
6. Wetting measurement 18
6.1. CA measurement 18
6.2. LEP measurement 19
6.3. Penetrating drop concentration method 20
6.5. Penetration temperature method 21
7. Membrane restoration 21
7.1. Rinsing and drying 23
7.2. Backwashing 23
8. Mathematical modeling of wetting 25
9. Membrane non-wetting characteristics 26
10. Effect of operating conditions on wetting 28
11. Effect of MD configurations on wetting 29
12. Approaches to control wetting 30
12.1. Pretreatment/Hybrid MD processes 30
12.2. Advances in membrane fabrication 34
12.2.1. Membrane surface modifications 39
12.2.2. Membrane bulk modifications 41
12.3. Flow effects of buoyancy 44
12.4. Operating conditions 45
12.5. Membrane surface barrier protection 45
13. Conclusions and perspective 46
References 49
Highlights 88
Graphical Abstract 88

1. Introduction

Membrane distillation (MD) is a thermally driven membrane separation process, which utilizes a microporous hydrophobic membrane that allows vapor to pass through it but not liquid. MD's driving force for the mass transfer is the transmembrane vapor pressure difference, which is induced by the transmembrane temperature difference or by reduction of vapor pressure on the permeate side by vacuum or dry gas (Carrero-Parreño et al., 2017; Lee et al., 2015). The volatile components present in the feed solution evaporate at the entrances of pores, and therefore the mass transfer through the membrane only takes place in the vapor phase (Kishor G Nayar et al., 2015; Politano et al., 2016; Swaminathan et al., 2016b).

MD offers several advantages and some potential applications based on the following benefits. MD operates at lower temperatures than the boiling point of the solvent, and therefore it can deal with temperature-sensitive solutions (e.g., in the food or pharmaceutical industries (El-Abbassi et al., 2013)). Since the vapor pressure is not highly dependent on the salt concentration, MD can be used in combination with reverse osmosis (RO) for the treatment of highly saline water (Warsinger et al., 2018).

Although MD is potentially attractive for some applications, it still suffers from a few drawbacks and has gained little acceptance industrially. These disadvantages include high-energy consumption compared to alternative membrane processes, and wetting phenomenon. The energy needs for MD can be provided if it integrates with renewable energy or available "waste" heat (David M. Warsinger et al., 2015) or solar thermal (Guillén-Burrieza et al., 2011), and new configurations and operating conditions continue to improve the energy efficiency of MD (Chung et al., 2016; Summers and Lienhard, 2013; J. Swaminathan et al., 2018; Swaminathan et al., 2016a, 2016c; David E.M. Warsinger et al., 2015). However, the incidence of membrane pore wetting due to the loss of membrane hydrophobicity for the feeds containing wetting compounds (e.g., oils, surfactants) is still challenging its industrial potential (Banat and Simandl, 1994; El-Bourawi et al., 2006; Qtaishat and Banat, 2013).

Penetration of feed solution into the membrane pores occurs if solutions with organic or/and inorganic compounds adsorb/deposit to the membrane surface or if the transmembrane hydrostatic pressure surpasses the liquid entry pressure. Pore wetting leads to either permeate flux reduction or permeate quality deterioration depending on the type of pore wetting. The former is the result of partial pore wetting, and the latter is as the consequence of full wetting.

A literature search for "membrane distillation" revealed more than 2180 records (through July 2017, in Scopus), with an escalating growth in the number of publications during the past decade (**Fig. 1**). In 1963, the first patent on MD was filed by Bodell (Bodell, 1963); however, the unavailability of adequate membranes for MD led to a lack of interest in MD for some time. Subsequent to the fabrication of porous polytetrafluoroethylene (PTFE) membranes by W. L. Gore and Associates, during the 1980s MD regained the attention of researchers. Nevertheless, research addressing wetting incidence and control wetting in MD remained minimal until recently. The entire number of published papers on MD is more than eleven times greater than that of MD articles exploring the wetting phenomena (2180 articles for MD and 171 for wetting in MD.

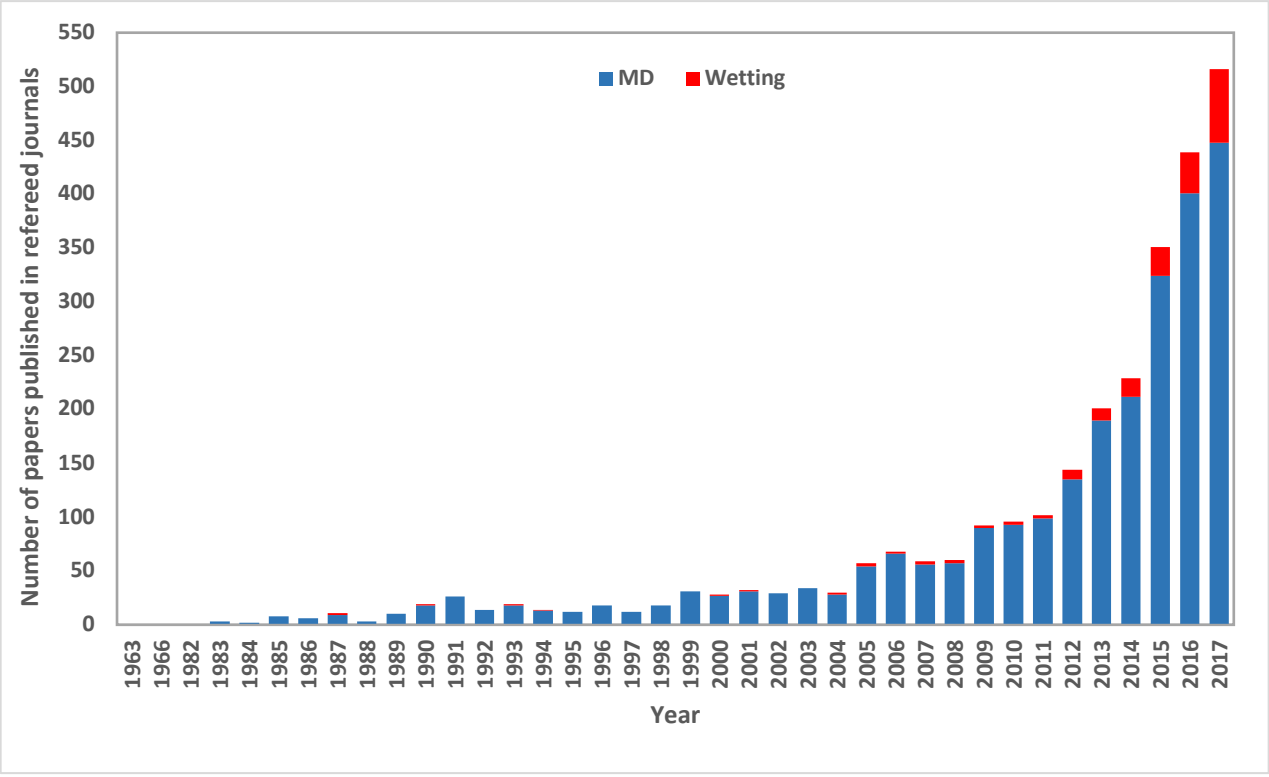

Fig. 1: The growth of research activity on MD and wetting phenomena, 1963-2016 (data from Scopus).

Today, wetting incidence in MD has gained more attention and more publications on MD investigate these phenomena, moving the field toward practical implementation. To the best of authors' knowledge, no comprehensive literature review has focused on the wetting phenomena in MD. This article provides an extensive literature review on the subject. The aim of this paper is to analyze the key wetting conditions, wetting types, harmful effects, and prevention techniques and to lay the groundwork for future technological advances.

2. Parameters for wetting

2.1. Liquid entry pressure

The primary metric for measuring membrane wettability is liquid entry pressure (LEP). The LEP of a solution (sometimes incorrectly called "wetting pressure") is the pressure (Pa) that must be applied to the solution before it goes through a dry membrane pore (Smolders and Franken, 1989). The maximum capillary pressure for a hydrophobic membrane depends on liquid surface tension, surface free energy and maximum pore size of the membrane. Based on the Young-Laplace equation (Young, 1807), LEP is defined as:

$$LEP = \frac{-B\gamma_l \cos\theta}{r_{max}} > P_f - P_p = \Delta P_{interface} \quad (1)$$

where P_f and P_p are the hydraulic pressure on the feed and permeate side, B is a pore geometry coefficient (Table 1), γ_l is the liquid surface tension, θ is the contact angle (CA) measured on the liquid side, where the liquid-vapor interface meets the membrane surface and r_{max} is the maximum pore size of the membrane (David M. Warsinger et al., 2016). This simple model is visualized in Fig. 2a and 2b. The θ for a water droplet on different surfaces is shown in Table 2.

Many membranes and process conditions can impact the LEP through the variables in Eq. (1), including operating temperature, solution composition, surface roughness, surface porosity, pore shape (i.e., pore radius and fiber radius (Ali et al., 2012; Guillen-Burrieza et al., 2015). For instance, Barbe et al. (Barbe et al., 2000) studied the effect of contact with a membrane with water and a $CaCl_2$ solution for 72 h on

membrane surface morphology. They found that the intrusion of water meniscus into large pores led to increase in the porosity, pore area, pore length and pore equivalent diameter, as well as pore spread factor of the membrane. As a result, the LEP of the membrane decreased.

Table 1: Pore geometry coefficient for different membrane pores

Type of membrane pore	Pore geometry coefficient	Reference
cylindrical pores	1.0	(David M. Warsinger et al., 2016)
elliptical or irregularly shaped pores	less than 1.0	(David M. Warsinger et al., 2016)
stretched membranes (e.g., PTFE) with small curvature radius	0.4-0.6	(Saffarini et al., 2013)

Table 2: Water contact angle (WCA) for different surfaces

Surface	WCA	Reference
Teflon	108° - 115°	(Alkhudhiri et al., 2012)
polyvinylidene difluoride (PVDF)	107°	
polypropylene (PP)	93.5°±0.2°	(Gryta, 2005)
ceramic membrane grafted with fluoroalkylsilanes	177°	(Khemakhem and Amar, 2011)
ceramic zirconia and titania membranes	160°	(Cerneaux et al., 2009)

Moreover, the utility of Eq. (1) for calculating LEP is limited because the CA and surface tension of feed may not be known for the system of interest. Therefore, Eq. (1) can be only used to interpret the experimental data (Lawson and Lloyd, 1997). Because membranes do not have cylindrical pores, the Purcell model was developed to describe the location of the pinning point of the liquid in the pores, using more realistic geometry (see Fig. 2d and e) than cylindrical assumed in Equation (1). The equation for LEP based on the Purcell model (Purcell, 1950) is

$$LEP = \frac{-2\gamma_l \cos(\theta + \alpha)}{r(1 + R/r(1 - \cos(\alpha))} \quad (2)$$

where R is the fiber radius and α is the angle below horizontal at which the liquid meniscus pins prior to breakthrough (Fig. 2). The value of α is calculated using the following equation:

$$sin(\theta + \alpha) = \frac{\sin\theta}{1 + r/R} \quad (3)$$

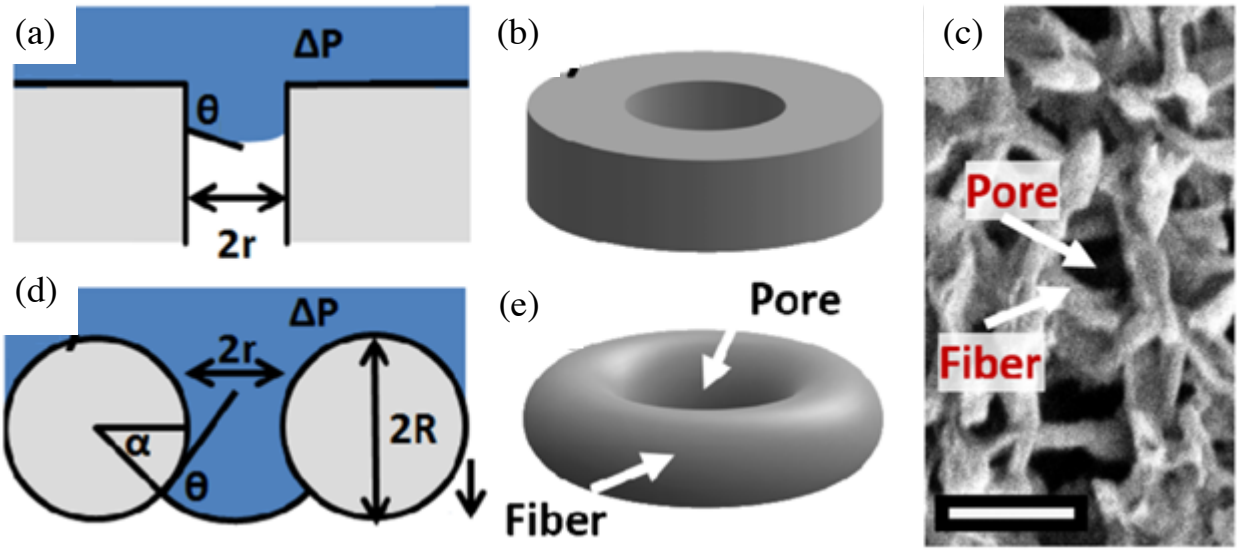

Fig. 2: (a) and (b) cylindrical pore (Young-Laplace model, Eq. (1)). (c) scanning electron microscopy (SEM) image of the nylon membrane (scale bar is 1 mm). (d) and (e) toroidal pore. Purcell model, Eq. (2) (Servi et al., 2016).

Unlike the Young-Laplace model, which predicts the LEP to be less than zero for all values of CA less than 90°, the Purcell model predicts positive values of LEP for all values of CA. However, this result is also in contradiction to the fact that many membranes wet at very low values of CA. Therefore, Servi et al. (Servi et al., 2016) developed a new model to predict the LEP for all values of CA considering the interactions between the liquid and the pores below the initially wetted surface by incorporating a "floor" below each pore into the model. This floor describes those fibers that may enable the liquid to penetrate further into the membrane. Therefore, LEP can be determined as the pressure at which the liquid separates from the pore or intercepts the floor, whichever takes place at the lower pressure. To calculate LEP using this new model, Eq. (2) is used along with Eq. (3) and the following equation

$$\frac{r + R\left(1 - \cos(\alpha)\right)}{-\cos(\theta + \alpha)}\left(1 - \sin(\alpha + \theta)\right) = R(1 - \sin(\alpha)) + h \quad (4)$$

where h is defined as the floor height (nm) describing the fibers that may attract the liquid to enter further into the membrane (Fig. 3). The modified model could explain the observed LEP performance over CAs ranging from 63° to 129°.

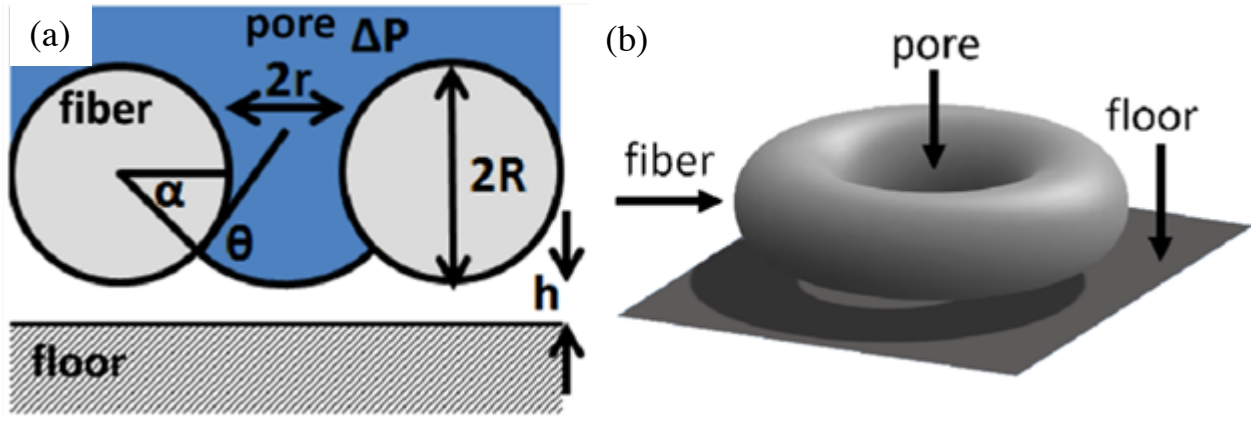

Fig. 3: The pore configuration for the Servi model, Eq. (4), from (a) the side; and (b) in three dimensions. h is the length between the bottom of the fibers and the floor. h can be positive or negative (Servi et al., 2016).

2.2. Membrane surface free energy

Surface free energy of a membrane (γ_m) is defined as the energy difference between the bulk and surface of a membrane. It can be estimated by measuring the receding CA (θ_r) and advancing CA (θ_a) of two liquid on the membrane surface using the two following equations (Owens and Wendt, 1969)

$$\left(1 + \frac{\cos\theta_a + \cos\theta_r}{2}\right)\gamma_l = 2\left(\gamma_m^d \gamma_l^d\right)^{0.5} + \left(\gamma_m^{nd} \gamma_l^{nd}\right)^{0.5} \quad (5)$$

$$\gamma_m = \gamma_m^d + \gamma_m^{nd} \quad (6)$$

where the superscripts *d* and *nd* correspond to the dispersive and nondispersive contributions to the total surface energy, respectively.

2.3. Surface wettability

The surface wettability is highly dependent on the free energy of the surface and its CA. In its simplest form, the wettability of a liquid droplet on a flat, smooth surface is commonly determined by Young's equation (Young, 1805):

$$\cos\theta = \frac{\gamma_{sv} - \gamma_{sl}}{\gamma_{lv}} \tag{7}$$

where θ is the CA in the Young's model, $\gamma_{lv}, \gamma_{sv}, \gamma_{sl}$ are the interfacial tensions liquid/vapor, solid/vapor, and solid/ liquid, respectively.

However, in reality, smooth surfaces are rare and some roughness is contained; therefore, the Wenzel's theory (Wenzel, 1936) was proposed where the roughness of the surface was considered for wettability determination.

$$\cos\theta_w = \frac{r(\gamma_{sv} - \gamma_{sl})}{\gamma_{lv}} \tag{8}$$

where θ_w is the apparent CA in the Wenzel mode and r is the surface roughness factor as the ratio of the actual solid/liquid contact area to its vertical projection. Based on Wenzel's theory, the liquid enters the grooves of micro-nano composite structure, and therefore this leads to higher CA on a rough surface than CA on a true flat surface (Fig. 4).

In Cassie's theory (Cassie and Baxter, 1944), the area fraction of solid and gas phase as a result of surface roughness contributes to the determination of wettability

$$\cos\theta_c = f_s \cos\theta_s + f_v \cos\theta_v = f_s(\cos\theta + 1) - 1 \tag{9}$$

where θ_c represents the apparent CA in the Cassie mode, taking into account that $f_s + f_v = 1$, $\theta_s = \theta$, and θ_v =180°. The Wenzel state and the Cassie state can be coexisting and transition between them can also occur (Lu et al., 2009). Change of the hydrophobicity toward superhydrophobicity is induced by air pockets, so-called "pillars" (Fig. 4c), between liquid and the surface generated by hydrophobic forces (Dumée et al., 2013; David E.M. Warsinger et al., 2015), therefore increasing the CA greater than 150° (Cao et al., 2009), reducing sliding angle (SA_{water}<10°) (Tijing et al., 2014a) and the surface free energy. Superhydrophobic

membranes made based on combined micro, and nanoscale roughness behave in Cassie-Baxter state and water droplet is easy to roll off.

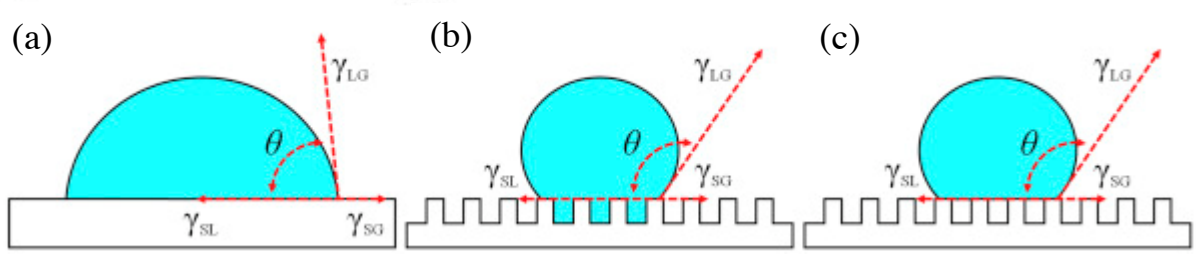

Fig. 4: Schematic representation of:(a) the Young model, Eq. (7); (b) the Wenzel model, Eq. 8; and (c) the Cassie-Baxter model, Eq. (9). The last of these best describes unwetted MD membranes (An et al., 2017).

3. Wetting mechanisms

Membrane pore wetting involves a complex of physical and chemical interactions (Alklaibi and Lior, 2005). The non-wetting liquid facing a hydrophobic membrane forming a fixed interface at the membrane pores was initially considered as one of the first principles of MD process by C. Gostoli et al. in 1987 [3]. They proposed that, based on capillary action, the non-wetting of a liquid is the result of its high surface tension forming a convex meniscus that impedes the liquid from entering the membrane pore. Therefore, the liquid feed in contact with membrane bulges in the pore until the pressure difference arising from the surface tension of the curved interface balances the pressure drop caused by the partial pressures of vapors and air across the membrane. The pressure caused by surface tension is called capillary pressure. When this pressure balance is overwhelmed, the liquid begins penetrating the pores. Once wetting takes place, the membrane starts to lose its hydrophobicity locally, leading to continuous water bridging.

Membrane wetting can be distinguished into four degrees (**Fig. 5**): non-wetted, surface-wetted, partially-wetted, and fully-wetted (Gryta, 2007a). Surface wetting shifts the interface of liquid/vapor inward of the membrane cross-section. Permeate flux may then decline gradually as a result of the associated increase in temperature polarization which lowers the temperature of the evaporating interface in the pore (Gryta, 2016a; Gryta et al., 1997). Although surface wetting even to a significant depth, e.g. 100–200 μm, still provides a liquid/vapor interface for separation, scaling as a result of solvent evaporation can take place

inside the pores in the vicinity of the meniscus (Gryta, 2007a). Moreover, crystal growth inside the pores accelerates scale formation rate by inhibiting diffusive transport of solutes and solvent between wetted pores and the feed bulk, raising solute concentrations locally. Conversely, under certain conditions, the intrusion of liquid into the pore has been observed to cause a temporary flux increase as a result of the shorter vapor diffusion path through the part of the pore that remains dry (Gilron et al., 2013). As feed solution penetrates deeper into the membrane pores, partial wetting can take place. In this case, the MD process can be continued if the majority of pores are dry. However, partial wetting under certain conditions can reduce the permeate flux due to a reduction of the active surface area for mass transport associated with partial wetting (blue solid line in Fig. 5) (Karakulski and Gryta, 2005) or it can cause an increase in the permeate flux due to wetting of some pores (i.e. vapor transport is overtaken by liquid transport) followed by a rapid decrease due to steady blockage of pores by the foulants depending on the experimental setup (blue dash line in Fig. 5) (Dow et al., 2017). The partial wetting also leads to deterioration of permeate quality. Interestingly, all the hydrophobic membranes used in MD, such as PP, PTFE, and PVDF, have shown partial wettability during a long-term use (Gryta, 2005). In the case of full wetting, the MD process no longer acts as a barrier, resulting in a viscous flow of liquid water through membrane pores, incapacitating the MD process (Rezaei et al., 2017a; Rezaei and Samhaber, 2016b). Fig. 5 shows qualitatively the permeate flux and rejection rate for an MD process based on the degree of wetting.

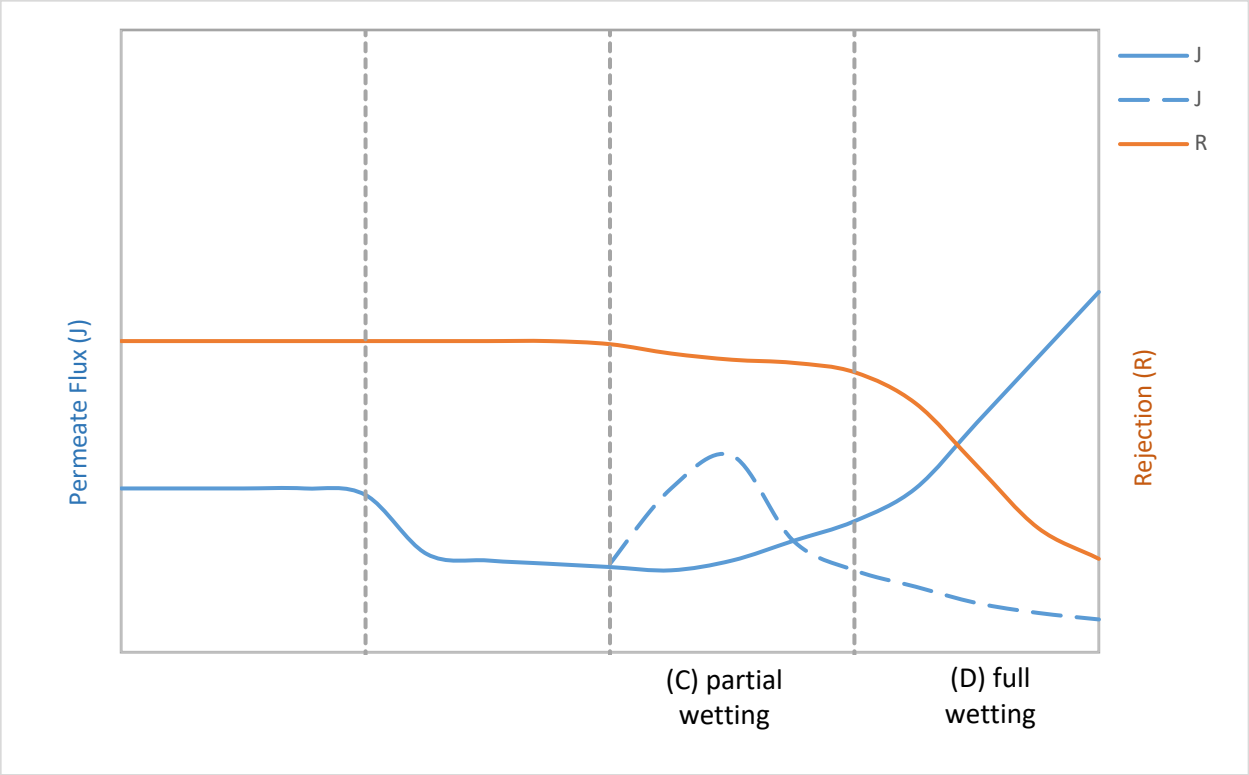

Fig. 5: Wetting degrees: (A) non-wetted; (B) surface-wetted; (C) partially-wetted; and (D) completely-wetted.

4. Wetting detection

Wetting is typically detected by evaluating the permeate quality. When membrane wetting occurs, the electrolyte solutes dissolved in the liquid feed penetrate into membrane pores, which leads to a significant increase of permeate electrical conductivity. This permeate quality change is frequently measured by permeate conductivity readings (Warsinger et al., 2017a). However as electrical conductivity increase also happens when volatile components such as ammonia and carbon dioxide pass through an intact membrane, wetting is detected occasionally by in-situ visual observation of the membrane (wetted membranes transition from opaque to transparent) (Dow et al., 2017), transmembrane pressure changes and membrane autopsy. Recently, Ahmed et al. (Ahmed et al., 2017) applied an electrically conductive layer to a direct contact membrane distillation (DCMD) combined with an electrochemical system to detect wetting (Fig. 6). The membrane acted as an electrode wherein the current through the system enabled Na^+ and Cl^- ions

to complete the cell. A constant voltage of +1V was applied during the MD process, and a quick increase in current was noticed at the moment where wetting occurred.

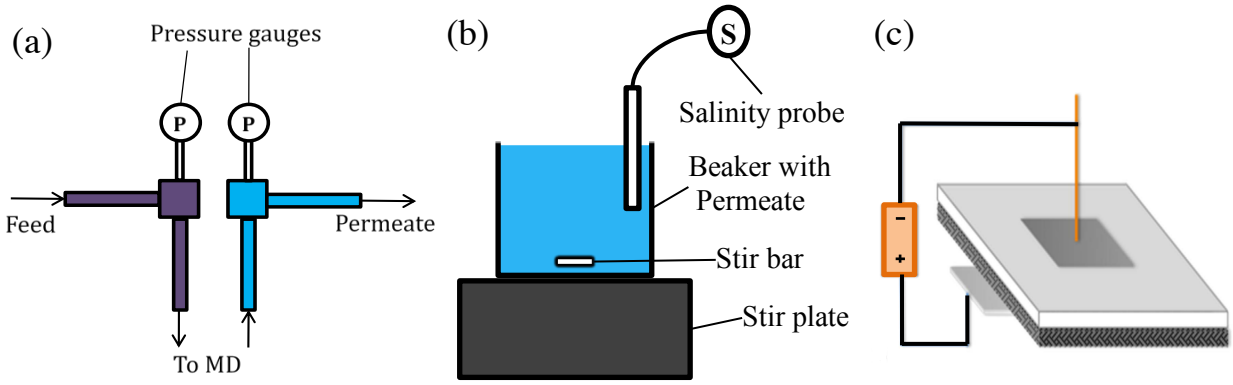

Fig. 6: Wetting detection mechanisms. a) measuring pressure changes across the membrane, reduced by leaks, b) measuring permeate conductivity, or c) electrochemical cell, where black is the electrically conductive carbon cloth layer, and white is the active electrospun PVDF-HFP (Ahmed et al., 2017).

5. Causes of wetting

The numerous causes of wetting in MD are detailed in Table 3. The primary cause of the wetting of MD membranes is fouling, meaning material deposition on the membrane surface and in membrane pores (Camacho et al., 2013; Gryta, 2007a; Hausmann et al., 2011; Tijing et al., 2015) . Other causes of wetting include surfactants which reduce the surface tension of the feed (Rezaei et al., 2017a), capillary condensation, and membrane damage (Ge et al., 2014; Lee et al., 2018). Different types of fouling in MD are distinguished by the deposited materials and include organic fouling (C. Liu et al., 2017; Mokhtar et al., 2016; Nguyen et al., 2017; Wu et al., 2016; Zarebska et al., 2014) such as biological fouling (or biofouling) (Wu et al., 2017; Zodrow et al., 2014) or fouling of organic compounds (Chew et al., 2014; Tan et al., 2016), and particulate or colloidal fouling (Ding et al., 2010; He et al., 2008; Qin et al., 2016; Zarebska et al., 2015), as well as scaling deposition (inorganic fouling). The deposits can reduce LEP as they are often hydrophilic, may damage the membrane (Guillen-Burrieza et al., 2013), and also clog the pores, which leads to a decline of permeate flux and permeate quality due to membrane wetting. Past studies have reviewed these foulants (D. M. Warsinger et al., 2015).

274 Table 3: Pore wetting causes and mechanisms in MD

Cause	**Mechanism**	**Reason**
Transmembrane pressure	Higher than LEP	Pressure spikes, operating with low surface tension fluids or large pore size membrane
Capillary condensation	Loss of temperature gradient	Temporary shutdowns or variable operating temperatures: these reduce the saturation pressure for vapor, causing condensation
Scale deposition (inorganic fouling)	Reducing the hydrophobicity of membrane	Deposition on surface and crystallization inside membrane pores
Organic fouling	• Reducing the hydrophobicity of membrane • Lowering the surface tension	• Forming attractive forces between hydrophobic materials within an aqueous system • Increasing the affinity of solution and membrane
Surfactants	Reducing the liquid entry pressure of the feed into the pores	The liquid entry pressure is linearly proportional to surface tension.
Membrane degradation during long-term operation	Formation of hydrophilic groups on membrane surface	Oxidative chemical or mechanical degradation

275 Besides the fouling, pore wetting can also occur when the hydraulic transmembrane pressure exceeds the
276 LEP. Chemical and mechanical degradation of the membrane are also considered to accelerate the
277 membrane wetting during long-term MD process. Gryta et al. (Gryta et al., 2009) reported that hydrophilic
278 groups on the membrane surface (e.g. hydroxyl (OH), carbonyl (C=O) and unsaturated (C=C) groups)
279 formed by chemical oxidative degradation of membranes could reduce the CA from 90° to 61.4°. The

following section discusses the MD wetting caused by inorganic and organic compounds more in detail (El-Bourawi et al., 2006). Weakly hydrophobic membranes are also known to gradually wet over time.

5.1. Inorganic fouling

Crystal growth of inorganic compounds (usually primarily consisting of calcium carbonate, calcium sulfate, and halite) on the surface of the membrane can reduce membrane hydrophobicity and eventually cause water logging due to partial wetting (Banat and Simandl, 1994; Bouchrit et al., 2015; Dah Y. Cheng and Wiersma, 1983; Gilron et al., 2013; M. Gryta, 2002; McGaughey et al., 2017; K.G. Nayar et al., 2015). This phenomenon has only been observed for the treatment of saturated solutions (Cho et al., 2016; Feng et al., 2016; Naidu et al., 2017; Sakai et al., 1988; Sanmartino et al., 2016) and not for diluted solutions (Li and Sirkar, 2004; Mericq et al., 2010; Song et al., 2007).

Extreme temperature and concentration polarization within the feed boundary layer can also result in the growth of minerals or salt crystals on the membrane surface and subsequently membrane scaling and wetting (Martínez-Díez and Vázquez-González, 1999; Meng et al., 2015b; Ruiz Salmón et al., 2017; R.W. Schofield et al., 1990; Warsinger et al., 2017b). However, Gryta (M. Gryta, 2002) observed that only NaCl salt deposits with a higher depth of 10 μm from the pore inlet for a membrane with a wall thickness of 400 μm could cause the pore wetting (Fig. 7).

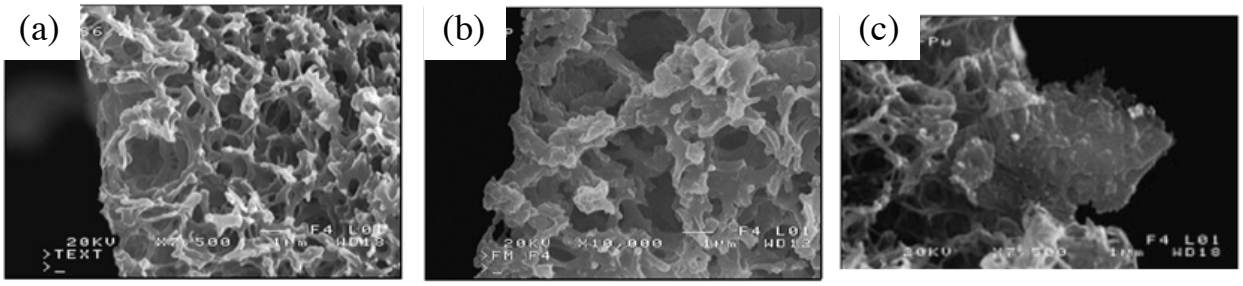

Fig. 7: MD scaling of NaCl crystals: shown here are SEM micrographs of a cross-section of Accurel PP S6/2 membrane demonstrating the pores on the feed side (inside the membrane capillary). a) Pristine membrane, b) after 138 h of MD integrated with salt crystallization, c) membrane with salt crystals inside the membrane pore (M. Gryta, 2002).

Importantly, MD membranes benefit from their hydrophobic surfaces, which have low surface energy and thus reduce crystal nucleation (David M. Warsinger et al., 2016).

5.2. Organic fouling

Organic compounds are particularly problematic for MD. When organic compounds are present in the feed solution, the surface tension of the solution decreases, and below a critical surface tension (i.e., surface free energy of the membrane), due to the high affinity of hydrophobic species such as oils to the hydrophobic membrane surface, wetting of the membrane may occur. In this respect, the chemical nature of the foulant (not the thickness) dictates the rate of wetting. For example, a thin layer of an amphiphilic fouling can reduce the CA of the membrane and result in wetting (Goh et al., 2013; Matheswaran and Kwon, 2007; Warsinger, 2015). Notably, while MD membranes are prone to wetting by organic compounds, they have been shown to experience less flux decline than RO or FO membranes undergoing biofouling (Jang et al., 2016).

Among different fouling types, growth of microorganisms can be significantly limited in MD due to high operating temperatures and feed salinity (e.g., in clean water production and desalination) (Marek Gryta, 2002a; Krivorot et al., 2011; D. M. Warsinger et al., 2015). However, organic foulants can contribute more to the wetting of hydrophobic membranes in MD (Naidu et al., 2015). Among organic foulants, surface-active compounds cause a major challenge in the technical implementation of MD (Soni et al., 2008). When a surfactant reaches a membrane surface, the hydrophobic membrane surface adsorbs the hydrophobic moiety while the hydrophilic part of the surfactant stays in the water phase (Chew et al., 2017a). Therefore, the hydrophobic surface is converted to a hydrophilic surface, resulting in a decreased CA and increased incidence of membrane wetting.

Notably, due to the hydrophobicity of MD membranes, solutes with lower surface tension can also cause wetting. For example, alcohols can cause membrane fouling and consequently pore wetting in MD due to the decrease of the surface tension of alcohol solutions, but their concentration plays an important role in the wetting occurrence. Table 4 summarizes the upper alcohol concentrations allowable in water for different membrane materials to avoid wetting.

Table 4: The upper alcohol concentrations in water for MD to avoid wetting

Alcohol	Maximum allowable alcohol concentration in water	Membrane	Reference
butanol	1.0 wt. % at 63°C 2.5 wt. % at 63°C	PP PTFE	(Kujawska et al., 2016)
ethanol	10.2 wt.%	PVDF	(Banat and Simandl, 1999)
ethanol	7 wt.% at 55°C	PTFE	(Shirazi et al., 2015)
ethanol	34 wt.%	PVDF with a mean pore size of 0.45 μm	(Treybal, 1980)

6. Wetting measurement

Hydrophobicity is determined by the interaction between the liquid and the membrane material. Immediate wetting in MD can be predicted by feed solution surface tension and water CA measurements (Lies Eykens et al., 2017). However, long-term performance tests are required to determine the non-wettability of the membrane with non-immediate wetting characteristics. The following section describes the common hydrophobicity measurements for membranes used in MD.

6.1. CA measurement

The conventional method to assess hydrophobicity of a membrane is CA measurement (Shaw, 1992). In this approach, the CA made by a liquid droplet on a membrane surface is measured by a goniometer, which determines relative wettability of membranes. The CA is obtained as the angle between the surface of the wetted membrane and a line tangent to the curved face of the drop at the point of three-phase contact (Onsekizoglu, 2012). The relative wettability of a membrane surface can be studied by measuring the receding and advancing angles of water on a membrane surface. The advancing water CA is associated with membrane hydrophobicity, and the receding angle is related the degree of molecular reorientation necessary to create a new equilibrium state with the aqueous solution (Khayet and Matsuura, 2004). The benefit of this approach is that the actual measurement is easy to perform (K. Y. Wang et al., 2008). However, CAs

can show hysteresis and are influenced by the surface structure (roughness) of the membrane (Adamson and Gast, 1997).

For CA determination, Neumann et al. (Kwok and Neumann, 1999) established an equation of state using Young-Laplace equation to relate the three interfacial tensions, which can predict the surface energy of a homogeneous dense polymer from surface tension and CA measurements for pure liquids

$$\cos\theta = -1 + 2\sqrt{\gamma_{SV}/\gamma_{LV}}\exp[-\beta(\gamma_{SV} - \gamma_{LV})^2] \quad (10)$$

where β is a parameter independent of the solid and the liquid. However, this model can just be applied for high values of surface tensions capable of generating obtuse CAs, thus implicitly excluding the critical zone where wetting occurs (Chibowski and Terpilowski, 2008). Courel et al. (Courel et al., 2001) modified Eq. (10) by introducing surface porosity of the membrane to improve the fitting quality of the model

$$\cos\theta^* = y^2\cos\theta - (1-y)^2 - 2y(1-y)\sqrt{\frac{\gamma_{SV}}{\gamma_{LV}} - \cos\theta} \quad (11)$$

where θ^* is the CA of a rough and hairy surface, $1-y$ is the surface porosity.

6.2. LEP measurement

The LEP depends on the interfacial tension of the feed, the CA of the membrane and the size, and structure of the membrane pores (Eq. (1)-(5)) (Franken et al., 1987; Rezaei and Samhaber, 2015, 2014). The LEP of a membrane can be measured by two approaches: static and dynamic method. The static LEP determination proposed by Smolder et al. is a variation of the bubble point method (ASTM International, 2014) (thoroughly described elsewhere (Smolders and Franken, 1989)). However, dynamic LEP measurement can be performed using a typical MD configuration (e.g., vacuum membrane distillation (VMD)). Similar to CA measurements, static LEP measurements have been considered to exhibit hysteresis (Bilad et al., 2015; Durham and Nguyen, 1994; Racz et al., 2015; Sarti et al., 1985). Moreover, this method has been abandoned because membrane compaction occurs during the test, which leads to higher LEP measurements (Durham and Nguyen, 1994). Notably, a recent study showed that this measurement could be improved by

measuring the rate of depressurization after stepwise pressure increase, rather than taking the maximum pressure value achieved (Warsinger et al., 2017a).

6.3. Penetrating drop concentration method

To determine the critical solute concentration in the penetrating drop method (Franken et al., 1987), a droplet with the particular concentration of organic material, which is on the verge of penetration into the membrane, is considered as the penetrating drop and the corresponding surface tension is the surface tension of penetrating droplet. The surface tension at which microporous membranes are wetted under process conditions can be calculated by the following equation:

$$\gamma_L = \gamma_L^P + \frac{\Delta P \, r_{max}}{2B} \tag{12}$$

where γ_L^P is the surface tension of penetrating liquid measured from penetrating drop method, ΔP is the applied pressure difference and B is a dimensionless geometrical factor. However, this approach can be used for membranes with a surface tension greater than 23 mN/m (Durham and Nguyen, 1994) as the liquid with lower surface tensions wet the membrane instantaneously.

6.4. Sticking bubble technique

In this method, a piece of membrane is placed horizontally at the bottom of the beaker containing a liquid with defined surface tension (Keurentjes et al., 1989). The air bubbles are brought into contact with the top surface by a flat-ended needle. Hydrophobicity is expressed in terms of the surface tension of liquid at which an air bubble has a 50% chance of detaching from the membrane surface ($\gamma_L = \gamma_d$). In the case where radius of bubble (R) is equal to radius of curvature at the top of the bubble (b), the following expression provides the CA of a spherical and deformed air bubble (Fig. 8):

$$\gamma_d = \frac{\Delta\rho g R^2 (\frac{2}{3} + \cos\theta_2 - \frac{1}{3}\cos^3\theta_2)}{2\sin^2\theta_2} \tag{13}$$

$$\sin\theta_1 = \frac{\Delta\rho g R^2 (\frac{2}{3} + \cos\theta_2 - \frac{1}{3}\cos^3\theta_2)}{2\,\gamma_d \sin\theta_2} + \sin\theta_2 \tag{14}$$

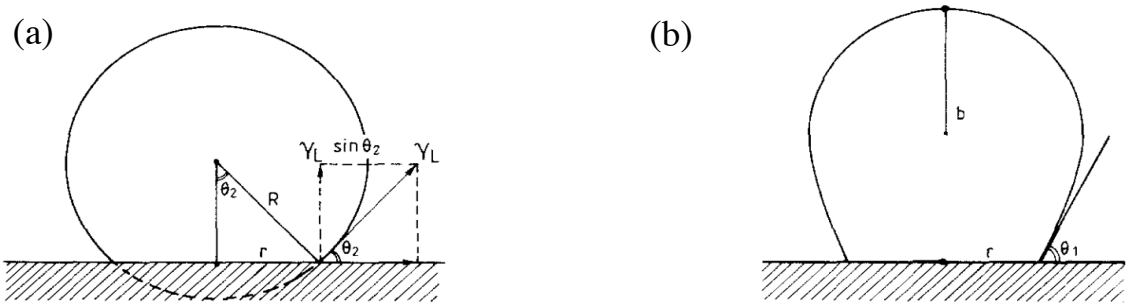

Fig. 8: The air bubble-liquid-membrane system for spherical (a) and deformed air bubbles (b).

6.5. Penetration temperature method

Penetration temperature method was developed for membranes with a surface tension less than 23 mN/m (Durham and Nguyen, 1994). In this approach, either propan-1-ol (*n*-propanol) or propan-2-ol (isopropanol) is placed into a test tube (10 ml at 15° C) with the membrane and thermometer. The test tube is sealed with Parafilm® and placed in a 35° C water bath. The test tube is gradually heated until bubbles appeared on the membrane, then the test tube is lightly tapped, and then the temperature increased at 1° C intervals. The penetration temperature measurement (PT° C) was recorded, when the membrane was almost transparent. The surface tension of the membrane was evaluated using following relationships:

$$\gamma_s = \text{PT° C} \times -0.0777 + 25.253 \qquad \textit{for Propan-1-ol} \tag{15}$$

$$\gamma_s = \text{PT° C} \times -0.0777 + 22.85 \qquad \textit{for Propan-2-ol} \tag{16}$$

7. Membrane restoration

Wetted membranes must be entirely dried and cleaned before subsequent usage (Tomaszewska, 2000), which leads to process downtime and potential membrane degradation (Guillen-Burrieza et al., 2013). On one hand, membrane regeneration in the MD process is challenging, and because in many cases fouling is associated with the membrane wettability (Marek Gryta, 2002b), the acquired results are not favorable. On the other hand, reducing the hydrostatic pressure below the LEP will not guarantee the restoration of membrane pores back to unwetted condition. This phenomenon is explained by Lawson et al. (Lawson and Lloyd, 1997) and illustrated in Fig. 9. As $\Delta P_{interface}$ is increased to LEP no liquid wets the membrane pores until LEP is reached (step 1). From this point on the liquid starts to penetrate into and flow through

403 the bigger pores as the pressure increases (step 2). Once all the pores become filled with the liquid, the flux
404 is governed by the Darcy's law ($J = K\Delta P$). Decreasing the pressure results in a linear decrease of flux (step
405 3). In order to restore the membrane to the initial conditions, the membrane needs to be dried. However,
406 solutes in the feed can be left inside the pores of the membrane after the evaporation of the solvent. In this
407 case, the membrane needs to be initially chemically cleaned and then dried in an oven.

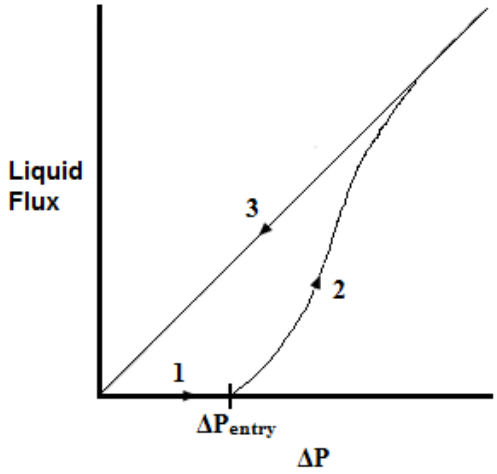

408

409 Fig. 9: Liquid flux versus transmembrane pressure difference (Lawson and Lloyd, 1997) (LEP = ΔP_{entry})
410 Periodic removal of fouling layer can also limit the gradual reduction of permeate flux in MD. Moreover,
411 stabilizing a thinner scaling layer on membrane surface by shortening the interval between the cleaning
412 operation is reported to reduce the risk of partial wetting due to the restriction of the degree of oversaturation
413 inside the wetted pores (Fig. **10**a and b) (Gryta, 2015). However, the dissolution of deposits can facilitate
414 wetting as a result of internal scaling (Fig. **10**c) (Chen et al., 2014a; Gryta, 2017, 2008).

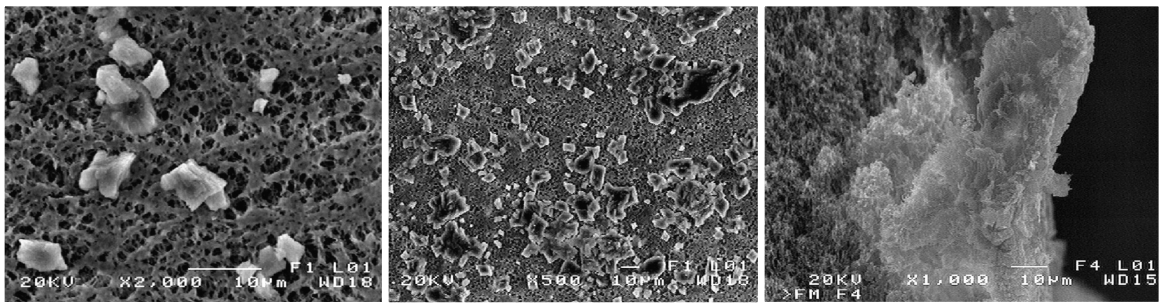

415

Fig. 10: SEM image of the membrane surface with deposit formed after (a) 1 h of MD process duration (b) 5 h of MD process duration. Feed: tap water (c) SEM image of capillary membrane cross-section. The crystallite formed inside the membrane pores (Gryta, 2015).

7.1. Rinsing and drying

Regeneration of membranes wetted by chemical membrane degradation via rinsing and drying has proved to be ineffective because of the presence of the hydrophilic groups on membrane surface (Gryta et al., 2009). He et al. (He et al., 2008) reported that the effective regeneration of wetted membrane could not be achieved by the process of rinsing the membrane with distilled water, and drying in the oven. This was due to deposition of salt crystals inside the pores and consequently, an irreversible structural change induced by the liquid intrusion inside the pores. Another attempt was also performed to remove the iron dioxide precipitates from the surface and pores of PP membrane with concentrated HCl solutions (Gryta, 2007b). The results showed that the complete removal of iron oxides from the capillary membrane (also including that precipitated into the pores) by rinsing caused wetting of some membrane pores leading to a reduction of permeate flux by 21%. In this case, the acid solution filled the pores adjacent to the pores filled by the deposit, which resulted in an increase of the area of the wetted membrane.

7.2. Backwashing

Another approach for membrane cleaning is backwashing. For instance, air backwashing of the scaled membrane can help to remove crystals and scales. However, when applied to a dried membrane, the effectiveness of this method is limited only for removal of deposits on at the membrane pore mouth (Choi et al., 2017). Backwashing with air is best when a wetted membrane still contains liquid: air pressures exceeding the liquid entry pressure can force wetting liquid out, keeping the solutes from precipitating. (D. M. Warsinger et al., 2016; Warsinger et al., 2017a). Shin et al. (Shin et al., 2016, 2015) explored the dewetting efficiency of high-temperature air on a wetted PVDF membrane. They found that the optimal condition for the air temperature and exposure time ranged from 60-70 °C and 8-12.5 min, respectively. UV irradiation has also been reported to partially clean the PVDF/TiO_2 superhydrophobic membranes fouled by gallic acid (Hamzah and Leo, 2017). Their results showed that the gallic acid foulants were

decomposed under the irradiation of UV light due to photocatalytic activity of TiO_2 nanoparticles blended in the membrane.

Recently, Warsinger et al. (Warsinger et al., 2017a) studied the effectiveness of pressurized air backwashing (PAB) relative to the membrane dryout to reverse membrane wetting in MD. They found out that PAB restored the LEP to 75% of the pristine membrane for lower salinity feeds by removing the saline solution from the membrane without separating water and salts by vaporization. Notably, this method did not involve a dryout step or evaporation (the air was cool), and thus provided dewetting in ~10 seconds of treatment. However, there remains a possibility that air backwashing can cause partial tears in the membrane structure (Fig. **11**).

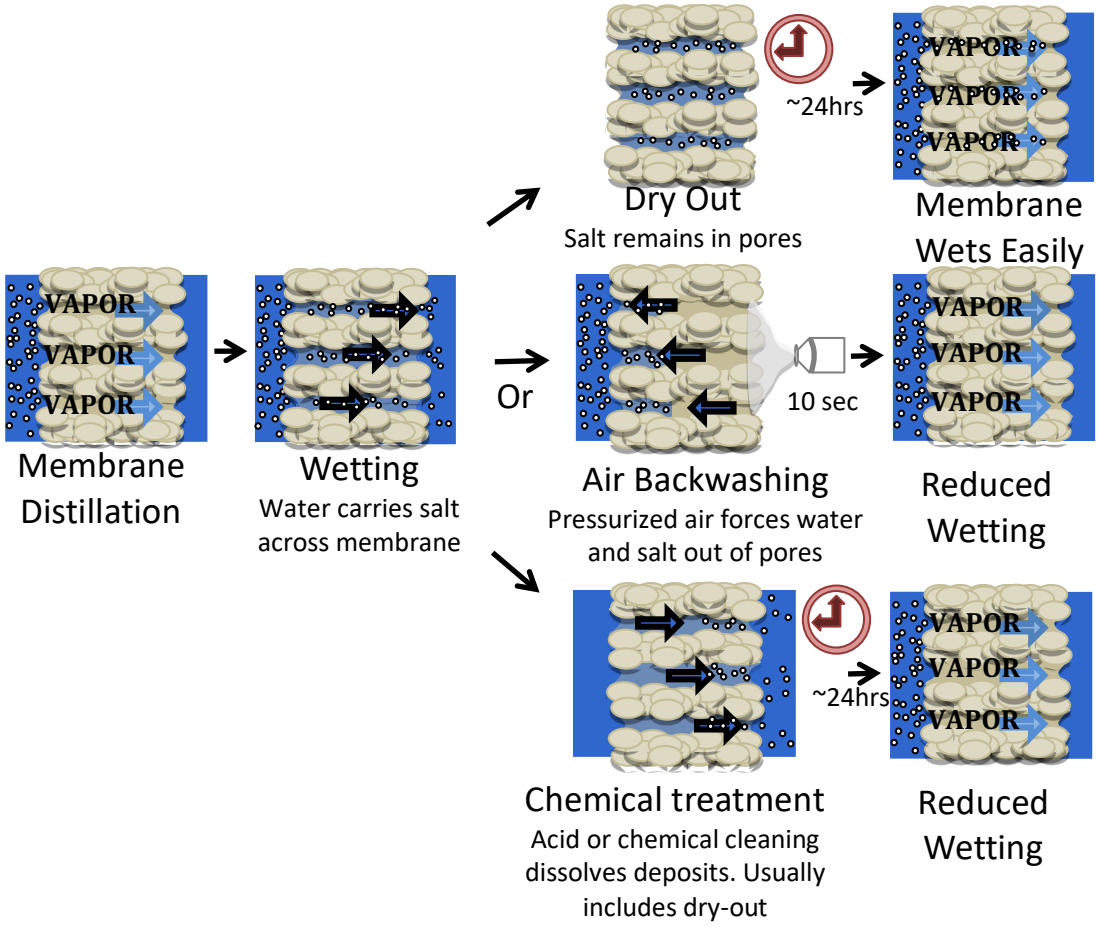

Fig. 11: Methods for wetting reversal, adapted from (Warsinger et al., 2017a).

8. Mathematical modeling of wetting

One of the main drawbacks in describing the wetting phenomenon in MD is the lack of mathematical models (Babalou et al., 2015). Membrane wetting behavior is complex to simulate, as it is mainly influenced by the microstructural characterization of the membrane itself (Dong et al., 2017). Peña et al. (Peña et al., 1993) proposed a MD model, which evaluates the decrease of permeate flux and steady-state pressure difference due to the progressive membrane pore wetting by the following equation:

$$J = non\ isothermal\ flux - hydraulic\ flux = (1-\alpha_i)B'\Delta T_b - \alpha_i A\Delta P_i \quad (17)$$

$$J_i = \frac{B'\Delta T_b\ A\Delta P_i^{st}}{B'\Delta T_b + A\Delta P_i^{st}} \quad (18)$$

$$\alpha_i = \frac{B'\Delta T_b}{B'\Delta T_b + A\Delta P_i^{st}} \quad (19)$$

where J is the net volume flux, at the arbitrary time of t_i, J_i is each of the measured fluxes (non-isothermal or hydraulic), B' is a measured or apparent non-isothermal phenomenological coefficient, ΔT_b is the temperature difference in the bulk phases, A is a permeability coefficient, ΔP_i^{st} is the steady-state measured pressure difference when the cold chamber is sealed, and α_i is the percentage of liquid-filled pores. Coefficients A and B' can be calculated based on a two-parameter non-linear regression method from the experimental pairs J_i and ΔP_i^{st} for a given value of ΔT_b. Following the model proposed by Peña, García-Payo et al. (García-Payo et al., 2000) proposed the following equations to calculate the LEP taking into account the axial irregularity of pores:

$$LEP = -\frac{2\gamma_L}{r_{max}}\frac{\cos\left(\arcsin(\xi)\right)}{\left[1+\frac{2R}{r}sin^{\,2}\left(\frac{\theta_A}{2}-\frac{\arcsin(\xi)}{2}\right)\right]} \quad (20)$$

where r is the mean pore radius, θ_A is the advancing CA, R is the mean curvature radius of pore wall elementand $\xi = \frac{\frac{R}{r}\sin\theta_A}{1+\frac{R}{r}}$ (Fig. **12**).

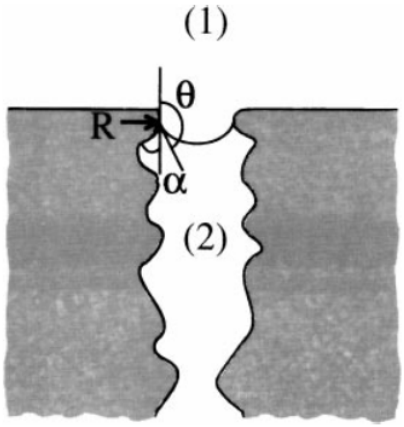

Fig. 12: Interface in an irregular pore of the hydrophobic membrane. (1) Liquid phase and (2) gas phase.

When the geometry of the pore is axially irregular, a structure angle, α, may be defined as the angle between a pore wall element and the normal to the membrane surface in the axial direction (García-Payo et al., 2000).

For polar or hydrogen bonding liquids on non-polar solids with low surface energy, the LEP can be calculated based on van der Waals dispersion components of the work of adhesion of a fluid to a solid surface (García-Payo et al., 2000):

$$LEP = \frac{2}{r_{max}}\left(\gamma_L - 2\sqrt{\gamma_S^d \gamma_L^d}\right) = \frac{2}{r_{max}}(\gamma_L - \gamma_L^w) \quad (21)$$

where γ_S^d,γ_L^d are the dispersion components of surface tension of the solid and the liquid and γ_L^w is the wetting surface tension (i.e., LEP=0).

9. Membrane non-wetting characteristics

The main prerequisite to be satisfied by the membranes during MD operation is that solutions on both sides of the membrane do not wet the pores of the hydrophobic membrane (Zydney, 1995). The question of how to characterize the wettability of a MD membrane is a critical one, although few structural studies can be found in the literature.

The selection of membrane material and properties can assist to prevent membrane wetting. In MD, intrinsic hydrophobic microporous polymeric membranes such as PVDF, PP, polytetrafluoroethylene (PTFE) and polyethylene (PE) are used. However, these membranes are prone to wetting if LEP is exceeded.

As the first prerequisite for a proper membrane operation under fluctuating pressures and temperatures in the plant, the LEP of the membrane is recommended to be higher than 2.5 bar regardless of the MD configuration (Eykens et al., 2016; Schneider et al., 1988a). A more hydrophobic membrane can decrease the chances of reduction of the permeate flux due to partial wetting. PVDF is a less hydrophobic polymer relative to other polymeric MD membranes. PVDF has a surface free energy of 30.3 mN/m while PE, PP, and PTFE membranes have surface free energies of 20-25 mN/m, 30 mN/m, and 9-20 mN/m, respectively (Ashoor et al., 2016; Bonyadi and Chung, 2007; Cheng et al., 2010). Therefore, PVDF membranes might be more prone to the wetting. However, PVDF membranes have been wildly used due to easy processability.

Moreover, the intrinsic CA of nonporous PVDF material is less than 90°. However, it can be enhanced by increasing the surface roughness (Kang and Cao, 2014). Compared to the hydrophobicity of the membranes, the surface roughness is more crucial than low surface energy. The reason is that when two surfaces with different hydrophobicity are roughened, both can become superhydrophobic (Tijing et al., 2014a).

Wetting concentration (i.e., the lowest concentration of a solution that wets the membrane spontaneously (García-Payo et al., 2000)) is always considerably higher for PTFE membranes than the wetting concentration for PVDF membranes under identical experimental conditions (An et al., 2016a; Courel et al., 2000; García-Payo et al., 2000). However, the utilization of PTFE in large-scale industrial applications is restricted due to its various disadvantages, such as a high fabrication cost and environmental impacts (Gryta, 2016b).

PP has a relatively high surface energy (29 mN/m) and the smallest CA among other polymers used in MD. These traits have been found to result in partial wetting after few weeks of operation in an MD process (Gryta, 2005).

Using membranes with a small pore size (maximum micropore radius of less than 0.6 μm and LEP more than 100 kPa (L. Eykens et al., 2017; Rao et al., 2014; Thomas et al., 2014)) and high tortuosity (i.e., 50-80%) as well as the sponge-like structure can ensure that process pressure and temperature fluctuations do not lead to membrane wetting (Kezia et al., 2015; Schneider et al., 1988b). Higher membrane porosities

than 80% are usually accompanied by large pore sizes which are not suitable as they intensify the danger of membrane pore wetting (Banat and Simandl, 1998). The use of a nonporous membrane in MD similar to pervaporation has been proposed since the dense structure of the membrane inhibits wetting (Purwasasmita et al., 2015).

The thickness of the membrane also plays a major role in wettability of the membrane. A decrease in membrane wall thickness significantly improves the permeate flux. However, it increases the risk of membrane wetting.

10. Effect of operating conditions on wetting

The operating conditions for MD can be controlled such that membrane wetting is prevented. For instance, pressure spikes or absence of temperature gradient can result in wetting of some pores and consequent deterioration in the quality of distillate (Peng et al., 2017; Walton et al., 2004). Membrane temperature decline due to membrane dry-out as the result of temporary shutdowns can precipitate dissolved substances from the feed on the membrane surface and pores, accelerating membrane wetting (capillary condensation (Atchariyawut et al., 2006; Meng et al., 2015b)). Therefore, for instance, in the case of intermittent operation, the proper shutdown protocols are needed when storing used MD modules for the extended periods of time (Guillen-Burrieza et al., 2014).

On the contrary, the surface tension of solutions decreases with an increase in temperature, making the wetting a greater challenge at higher temperatures (Nayar et al., 2014). For pure water, the value of surface tension varies between 72-64 mN/m for temperatures between 25-70°C. Increasing feed temperature can also increase the scaling and membrane wetting due to oversaturation in the boundary layer for the saturated brine solutions (Edwie and Chung, 2013; Ge et al., 2014; Shirazi et al., 2014). The sustainability of a DCMD process for a hypersaline solution at a higher temperature difference of 40 °C was compromised due to membrane wetting (Hickenbottom and Cath, 2014).

Lowering the applied pressure in the feed and the permeate through adjusting the feed and permeate flow rates reduces the pressure difference across the membrane, hence reducing the tendency for the membrane wetting due to operating below LEP (Luo and Lior, 2017; R W Schofield et al., 1990). Moreover, permeate

quality deterioration can be avoided if the permeate pressure is kept higher than the feed pressure. Therefore, the feed cannot directly flow through the wet pores to the permeate side. In this case, MD process may be continued; however, after a wetting incident, the permeate flux decreases due to the reduction of active pores. In DCMD, a slightly higher pressure on the permeate side than the feed side has been used to reduce the risk of wetting (Zakrzewska-Trznadel et al., 1999).

Although high cross-flow velocity minimizes the boundary layer resistances and leads to higher permeate flux, it increases the pressure difference across the membrane (e.g., 10-20 kPa) and enhances the risk of pore wetting. Thus, the recirculation rate should be high enough to reduce the polarization effect, and sufficiently low to operate below LEP (Lawal and Khalifa, 2015; Naidu et al., 2014; Srisurichan et al., 2006; Y. Zhang et al., 2015). In this case, the feed flow rate must be varied with due precautions as the transmembrane hydrostatic pressure which needs to be always lower than LEP is a function of the second power of the feed velocity.

Recently, Guillen-Burrieza et al. (Guillen-Burrieza et al., 2016) conducted DCMD experiments to understand the effect of operational parameters on the wetting phenomenon and concluded that when parameters are adjusted in a way that increases permeate flux, both the wetting time and rate are reduced. Notably, feed and permeate temperatures are more associated with the wetting time (e.g., high ΔT increases the wetting time), while feed and permeate flow rates are more influencing the wetting rate (the lower one decreases the wetting rate).

Additionally, it is important to note that numerous operating factors that increase fouling also may increase wetting. These factors imply the need for avoidance of stagnation zones from spacers or piping that give time for crystal nucleation, avoidance of high-energy surfaces (e.g. metals) which may induce nucleation, and implementation of proper pretreatment for fouling particles (Warsinger et al., 2017b).

11. Effect of MD configurations on wetting

As the feed conditions can vary independently of configuration, in most cases the configuration impacts wetting little. Particular attention must be noted in VMD to avoid membrane wetting because in this configuration vacuum is applied to the permeate side and therefore $\Delta P_{interface}$ is usually higher in VMD

than in the other MD systems (Hassan et al., 2015; Lawson and Lloyd, 1997; Mohammadi and Akbarabadi, 2005). Therefore, the VMD has been used just for removal of volatile organic compounds from dilute aqueous solution and, unlike other membrane processes such as pervaporation, not for separation of organic/organic or organic/water mixtures. Notably, process conditions influenced by configuration choice can have an impact on wetting, such as temperature differences at the membrane surface (which impacts foulants and also surface tension), and concentration polarization caused by greater flux. In a study conducted by Meng et al. (Meng et al., 2015a), membranes in submerged VMD (with no agitation) were wetted quickly within the first 8 h of inland desalination operation, whereas membranes in cross-flow VMD maintained rather low permeate conductivity for 50 h.

12. Approaches to control wetting

Different approaches to control wetting in MD have been proposed by several researchers. Most of the emphasis has been on advancement in membrane fabrication in such a way to ensure a low affinity between the liquid and the polymeric material. This has been mainly done through modifying the membrane surface geometrical structure and surface chemistry. Several studies also investigated the integration of filtration processes with MD as pretreatment steps. The following section reviews these approaches in more detail.

12.1. Pretreatment/Hybrid MD processes

Wetting of the hydrophobic membrane can be avoided by the use of a robust pretreatment of the feed liquid. Many of these processes effectively removed membrane wetting agents before they reached the membrane. However, one should note that the capital and operating costs of the process will increase due to the addition of a pretreatment step.

Several methods are proposed to be integrated with MD for different applications (Table 5). Integration of filtration processes with MD can remove most contaminants and foulants from the feed solution, thus mitigating the wetting problem. In the case of protein as a fouling agent, either the feed solution can be boiled followed by filtration to reduce the precipitation of proteins on the membrane surface (Gryta, 2008), or ultrasonic waves can be introduced to mitigate protein fouling (i.e., the deposition of bovine serum albumin aggregates) and consequently wetting incidence (Hou et al., 2017). Nanofiltration can also be used

591 to remove less soluble compounds including divalent salts (Roy et al., 2017): this has been integrated into
592 membrane distillation (Kumar et al., 2017). Ultrasonic treatment in a hybrid process with MD can also
593 mitigate membrane $CaSO_4$ scaling and thus reducing the risk of membrane wetting (Hou et al., 2015).
594 Additionally, coagulation pretreatment to form bigger crystals than the membrane pores can considerably
595 minimize the risk of scale formation inside the membrane pores. Accelerated precipitation softening
596 including pH adjustment with sodium hydroxide along with calcite seeding, followed by microfiltration to
597 avoid clogging by the seeds was integrated before DCMD to desalinate a primary RO concentrate (Qu et
598 al., 2009). Membrane distillation bioreactors (MDBR) couple thermophilic bioprocess, which results in
599 the biological removal of high concentrations of organics and nutrients. This pretreatment expands the
600 application of MD to the reclamation of industrial wastewater containing a low volatile solute content.
601 Another way to reduce scaling incidence in MD is chemical conditioning of the feed using antiscalants
602 (e.g., polyacrylic acid). The use of antiscalant could prolong the induction period for the nucleation of
603 gypsum and calcite, respectively; and slow down the precipitation rate of crystals (He et al., 2009; Peng et
604 al., 2015; P. Zhang et al., 2015). However, high dosing of antiscalant can also increase the risk of membrane
605 wetting because of organic nature of antiscalants. Most recently, Dow et al. (Dow et al., 2017) demonstrated
606 that the MD testing on a textile mill effluent that was first treated by flocculation and anaerobic/aerobic
607 digestions eliminated the wetting issue.

608 Table 5: Pretreatment process applied for MD to control wetting occurrence

Pretreatment	Process	Application	Impact	Results	Ref.
Physical	Ultrafiltration	concentration of grape juice	protein removal	max ~7% increase in juice surface tension	(Bailey et al., 2000)
	Microfiltration	ammonia stripping from pig manure	protein removal	2-4 times increase in ammonia mass	(Zarebska et al., 2015)

				transfer coefficient	
	Forward osmosis	wastewater reuse	ammonium, COD, arsenic removal	>99% removal efficiency of the volatile contaminants	(Husnain et al., 2015)
		real domestic wastewater treatment	removal of most high molecular weight contaminants	>90% removal efficiency of the organic matters, calcium salts, magnesium salts, sodium salts, silicates	(Li et al., 2018)
	Integreatd crystallization	shale gas produced water treatment	reducing scalant loading of multivalent ions, such as barium and calcium	increasing the total water recovery from 20% to 62.5%	(Kim et al., 2016)
	Multi-stage flash distillation	desalination of rejected brine	reducing concentration of different organic and inorganic contaminants	4-12% less reduction in permeate flux	(Kayvani Fard et al., 2016)

	Activated carbon	seawater and concentrated brine treatment	remove particulates and organic contaminants	21% and 23% removal of the antiscalant and antifoam agent	(Minier-Matar et al., 2014)
	Foam fractionation	concentrating textile mill effluent	capturing surface-active materials	increase of concentration factor from 27 to 34-fold	(Dow et al., 2017)
Chemical	Coagulation	desalination of recirculating cooling water	elimination of total organic carbon, total phosphorus substances	23% increase in permeate flux	(J. Wang et al., 2008)
	Chemical conditioning	treatment of RO brine	removing calcium hardness and sulfate ions	increase of final rejection factor form 58.6% to 97.9%	(Sanmartino et al., 2017)
Biological	Integrated bioreactors	reclamation of industrial wastewater	biological removal of organics and nutrients	delaying wetting by 1.7–3.6 times	(Goh et al., 2013)
	Biological treatments	textile wastewater treatment	digesting surfactants	reduction of TOC from 100 to 26 mg/L	(Dow et al., 2017)

Other	Microwave-assisted photo-catalysis	treating the coal gasification wastewater	preventing organic fouling by photodegrade the organic matters	increase of normalized permeate flux from 79.8% to 98.5%	(J. Wang et al., 2016)

12.2. Advances in membrane fabrication

Preventing and controlling membrane wetting via appropriate membrane design is of significant interest. Nevertheless, at present, most of the developed membranes still undergo some level of wetting. The current MD membrane design process relies heavily on commercial MF membrane fabrication methods, i.e., conventional thermal or dry/wet phase inversion techniques (Tijing et al., 2014a). These manufacturing methods lead to a non-homogeneous pore size distribution, which increases the risk of wetting for larger pores.

The primary goal of advancement in membrane fabrication is to obtain a surface with special non-wettability (Z. Wang et al., 2016a). These surfaces are categorized to superhydrophobic surfaces repellent to water, superoleophobic surfaces repellent to oil and omniphobic surfaces repellent to both water and oil. However, these methods commonly demand complex fabrication processes or high-specialized equipment, making them unacceptable inefficient production (Yang et al., 2016). Finally, the durability and long-term stability of these membranes are also questionable and require systematic research especially against high salinity feeds and different organic foulants (El-Bourawi et al., 2006; Yang et al., 2014; Zhang et al., 2005, 2013a).

Based on the goal of excellent liquid repellency, different strategies are developed to fabricate membranes with special non-wettability. Some of the methods developed to change not only the surface of the membrane but also the membrane matrix characteristics, while others are based on the physical and chemical modifications of surface morphology and microstructure of the fabricated membrane. The main disadvantages of the surface modification techniques are to change the membrane surface wettability

without affecting the bulk wetting properties. Superhydrophobic surface coating of the hydrophobic membranes increases the surface roughness and consequently the CA, θ as the contact angle in Eq. (1), but it can have less effect in increasing the LEP. The reason is that CA is a surface property only, while the LEP is affected not only by surface wettability of the membrane but also by the wettability inside of the pores. For example, according to Eq. (4), LEP is affected not only by the surface property but also "*h*", the floor height describing the interactions between the liquid and the pores below the initially wetted surface (Fig. 3). (Franco et al., 2008; Liao et al., 2013; Prince et al., 2013; Yan et al., 2017). As by surface coating in case of membrane surface wetting, fewer resistances exist inside the pores, and the liquid penetrates more easily throughout the membrane thickness (Jin et al., 2008). Therefore, both surface and bulk modifications are necessary to create the membrane in a designed way, and this cannot be accomplished solely by the structuring of the surface or only by chemical functionalization (D.Y. Cheng and Wiersma, 1983; Kujawa et al., 2017). Table 6 summarizes the applied methods for advancement in membrane non-wettability to increase the membrane hydrophobicity or providing anti-sticking/self-cleaning surfaces.

Table 6: Methods applied in MD for wetting prevention

Approach	Method	Inference	Reference
Membrane fabrication	incorporation of hydrophilic nonporous layers	to inhibit a transport of amphipathic molecules, however, includes more resistance than a porous hydrophobic coating	ethylene glycol (Chong et al., 2016; Majidi Salehi et al., 2016) polyvinyl alcohol (Z.-Q. Q. Dong et al., 2015; Mansouri and Fane, 1999; N.M. Mokhtar et al., 2014; Ray et al., 2017) polyethylene glycol (Feng and Jiang, 2006; Zuo and Wang, 2013) alginate (Xu et al., 2004)

			alginic acid-silica (Xu et al., 2005b) alginate-carrageenan (Xu et al., 2005a) chitosan (Chanachai et al., 2010)
	Loading of perfluorinated polymers	to increase membrane hydrophobicity by reducing surface free energy	(Chen et al., 2015; Edwie et al., 2012; Figoli et al., 2016; Guo et al., 2015; Kujawa et al., 2016; Lalia et al., 2013; Prince et al., 2014b; Tong et al., 2016; Xu et al., 2017; Y. Zhang et al., 2017; Zhao et al., 2017)
	loading of functionalized hydrophobic nanoparticles/nanofibers	to maximize membrane hydrophobicity by increasing the membrane CA and minimize the surface pores size	(Baghbanzadeh et al., 2015; Boo et al., 2016; Z.-Q. Dong et al., 2015; Dong et al., 2014; Efome et al., 2016; Fan et al., 2017; González-Benito et al., 2017; Hammami et al., 2016; Hamzah and Leo, 2017; Lalia et al., 2014; E.-J. Lee et al., 2017; Li et al., 2014a, 2014b, X. Li et al., 2016, 2015; T. Liu et al., 2016; K.-J. Lu et al., 2017; X. Lu et al., 2017, 2016; Ma et al., 2009; Moradi et al., 2015; Qing et al., 2017; Rezaei and Samhaber,

			2016b, 2016c; Su et al., 2017; Tijing et al., 2014b; Z. Wang et al., 2016b; Yan et al., 2017; W. Zhang et al., 2017; Zhong et al., 2017)
	loading of carbon-based micro- and nanomaterials	to enhance the membrane surface roughness	carbon nanotubes (CNTs) (Fan et al., 2016; J.-G. Lee et al., 2017; Y. Li et al., 2015; Mapunda et al., 2017; Okiel et al., 2015; Silva et al., 2015; Tijing et al., 2016; Woo et al., 2016a, 2016b) graphene (An et al., 2017; Moradi et al., 2015; Y. Wang et al., 2017; Woo et al., 2016a)
Membrane modification	Physical modification	to increase membrane surface roughness	plasma treatment (Chul Woo et al., 2017; Dumée et al., 2016; Fane et al., 2012; Li and Sirkar, 2005; L. Liu et al., 2016; Sirkar and Qin, 2001; Tian et al., 2015; Xu et al., 2015; Yang et al., 2014, 2015; X. Yang et al., 2011) layer-by-layer assembly (Arafat et al., 2015; N. M. Mokhtar et al., 2014; Prince et al., 2014b; Rezaei and Samhaber, 2016a; Tijing et al., 2014b; Woo et al., 2015; W. F.

			Yang et al., 2011; Zhu et al., 2015; Zuo et al., 2017) template replication (Peng et al., 2013) phase separation (Thomas et al., 2014; Xiao et al., 2015) electrospinning (An et al., 2016b; Huang et al., 2017) double re-entrant cavities (Domingues et al., 2017) thermal treatment (Shaulsky et al., 2017; Wang et al., 2014; Yao et al., 2017)
	Chemical modification	to reduce surface free energy	incorporation of surface-modifying molecules or low surface tension functional groups (Chua et al., 2015; Huang et al., 2016; Kujawa and Kujawski, 2016; Kujawski et al., 2016; Kyoungjin An et al., 2017; E.-J. J. Lee et al., 2016; K. J. Lu et al., 2016; Prince et al., 2012; Y. Wang et al., 2017; Wang and Lin, 2017; Xiaoxing et al., 2011; Yin et al., 2017; Zhang et al., 2013b; Zuo and Chung, 2016)

644 Some of these techniques have disadvantages. Generally, adding layers to a membrane surface reduces
645 permeability. Ideal MD membranes are highly porous with low conductivity, so denser regions may impair
646 system-level performance (Swaminathan et al., 2018). Added cost in fabrication is also another concern,
647 especially in steps that require long durations or expensive precursors. Importantly, many of the most
648 hydrophobic compounds ideal for MD membrane anti-wetting have environmental toxicity concerns (e.g.
649 fluoropolymers). Some processes (e.g., plasma coating) may damage some substrates, and so should be
650 chosen carefully. Finally, while increasing surface roughness can increase hydrophobicity, surface
651 roughness can have complex interactions with certain foulants, with increased adherence in some situations.
652 The following part of this section reviews some of the new aspects of advancement in membrane fabrication
653 methods for higher wetting resistance in MD.

654 **12.2.1. Membrane surface modifications**

655 As mentioned, the surface chemistry and geometrical structures determine the wetting property of
656 membrane. Surface chemistry adjusts the surface tension at the microscopic level, but geometrical structure
657 controls how these forces act upon the liquid (McHale et al., 2004). Thus, varying one of these two
658 parameters can regulate the surface non-wettability. The functionalization with low surface energy
659 materials particularly fluorosilanes (Fig. 13) can decrease the surface free energy. Alternatively, generating
660 a hierarchical nanostructure surface morphology with multi-level surface roughness can tune the surface
661 wettability (Razmjou et al., 2012). Moreover, increasing the surface roughness via nano-coating not only
662 contributes in engineering the hierarchical structure but also provides sites (OH functional groups) for the
663 hydrolyzed silane coupling agent to be anchored forming a robust uniform water-repellent film (Meng et
664 al., 2014a).

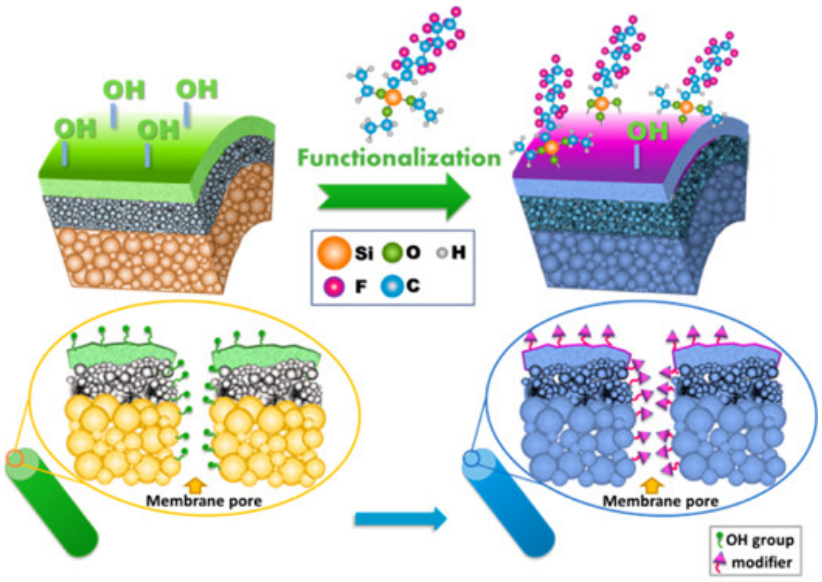

Fig. 13: The scheme of membranes functionalization by perfluoroalkylsilanes molecules (Kujawa et al., 2017).

Although the achievement of superhydrophobic membranes with these strategies is successful, most of the superhydrophobic surfaces are prone to wetting by organic solutions, and very few attempts are made to fabricate omniphobic membranes that provide enhanced repellency to different liquids such as oils and alcohols. Omniphobic membranes with a re-entrant structure provide a local kinetic barrier for shifting from the meta-stable Cassie-Baxter state to the completely wetting Wenzel state for low surface tension liquids. However, the main difficulties in fabricating stable omniphobic membranes for MD applications are the control of faultless and tedious surface topography and complicated fabrication procedures which are too expensive to be implemented in the large scales (Wei et al., 2016). On the other hand, applications of these membranes for the treatment of oily wastewater with all main components and the interaction between these elements via simulations tools are not deeply studied (Han et al., 2017). Until now, only a few reports studied the omniphobicity for non-polar liquids by developing specially designed patterns such as overhang structures, re-entrant curvatures, silicone nanofilaments and candle soots or by using inherently textured substrates (Brown and Bhushan, 2016; Darmanin and Guittard, 2013; Grynyov et al., 2016; Joly and Biben, 2009; Kota et al., 2013; Kota and Tuteja, 2012; L. Li et al., 2016; Song et al., 2013; Tuteja et al., 2007, 2008). Among these works, Lin et al. (Lin et al., 2014) developed the omniphobic microporous membrane

683 for MD that repels both water and low surface tension liquids by coating a hydrophilic glass fiber membrane
684 with silica nanoparticles, followed by subsequent surface fluorination and polymer coating (Fig. **14**). The
685 9 h course of DCMD experiments for the feed solution containing 1.0 M NaCl and 0.4 mM SDS at 60 °C
686 no wetting occurred for the omniphobic membrane, while for the PTFE membrane wetting became
687 progressively more severe as water flux increased more than fivefold and salt rejection dropped to 40% at
688 0.4 mM SDS. However, it is worth noting that the fluorinated chemicals are potentially dangerous and they
689 are regarded as persistent and global contaminants. New non-chemical methods such as pretreatment
690 methods or other physical water treatment techniques to prevent wetting are required to be evaluated. In
691 another study, Lee et al. (J. Lee et al., 2016) fabricated omniphobic nanofiber membranes by preparing
692 positively charged nanofiber mats and grafting negatively charged silica nanoparticles and fluoroalkylsilane
693 to achieve multi-level re-entrant structures. Their fabricated membrane showed wetting resistance to
694 various liquids, including ethanol with a surface tension of 22.1 mN/m and exhibited a stable desalination
695 performance for eight-hour operation.

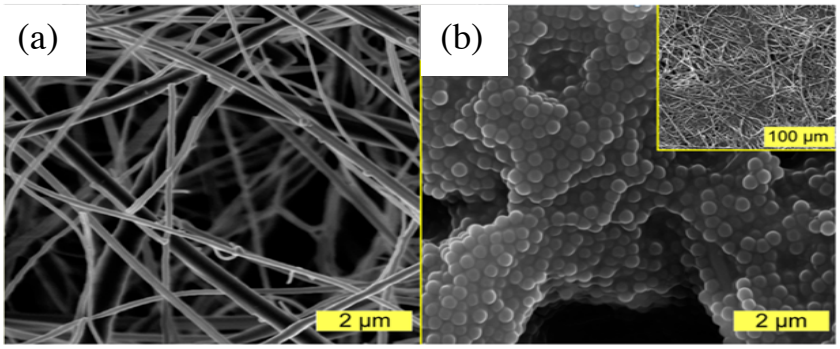

696

697 Fig. 14: SEM images featuring the local morphology of (A) a glass fiber (GF) membrane and (B) an
698 omniphobic membrane after the five-step modification procedure. The inset image in B shows the
699 morphology of a large piece of the omniphobic membrane (Lin et al., 2014).

700 **12.2.2. Membrane bulk modifications**

701 Membrane morphology and crystalline composition have a high impact on the wetting action of a
702 membrane. Formation of finger-like macro-voids in the polymeric membrane matrix due to the type of
703 solvent used in the fabrication process can reduce the LEP and therefore increase the risk of membrane

wetting (Fig. **15**). In the wet/dry spinning technique for fabrication of PVDF membranes, faster solvent/ nonsolvent exchange rate is responsible for the formation of finger-like structure or even macro-voids (García-Fernández et al., 2014). Blending PVDF and PTFE to form a sponge-like membrane structure is proved to be an effective way to increase membrane hydrophobicity (i.e., CA) (Gryta and Barancewicz, 2010). Fabrication of dual-layer membrane comprising finger-like and sponge-like layers can reduce the wetting risk while enhancing the membrane performance in regard to permeability. Wang et al. (Wang et al., 2011) demonstrated that the PVDF dual-layer hollow fiber with a fully finger-like inner layer and an entirely sponge-like outer-layer resulted in 98.6 L m^{-2} h^{-1} permeation flux and LEP of 0.7 bar.

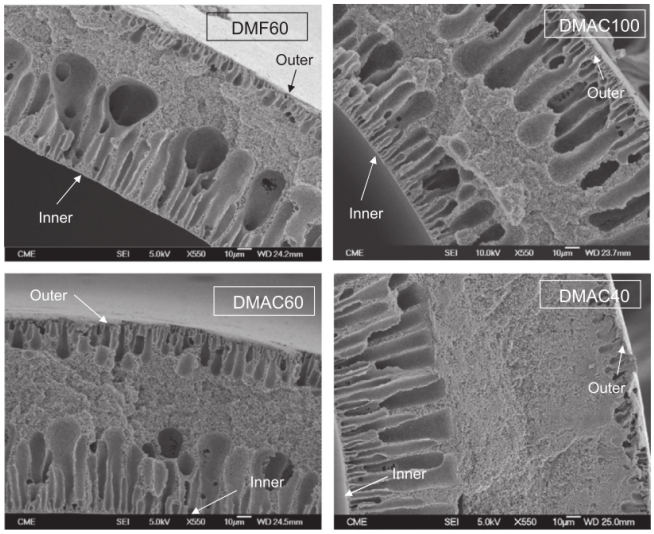

Fig. 15: SEM images of the cross-section morphology of the PVDF-HFP hollow fiber membranes prepared with different solvents (García-Fernández et al., 2014). All the membranes exhibit a sponge-like structure in the middle layer and a finger-like structure in the internal and external layers of the hollow fiber membranes.

A number of theoretical and experimental works have considered the composite hydrophilic/hydrophobic membranes for MD, but few have studied the wetting behavior of these membranes (Bilad et al., 2015; Feng et al., 2017; Gryta and Barancewicz, 2010; Jeong et al., 2014; X. Lu et al., 2016; Meng et al., 2014b; N. M. Mokhtar et al., 2014; Mostafa et al., 2017; Prince et al., 2013; Rezaei and Samhaber, 2016a; Tong et al., 2016; Zhu et al., 2015). Among these works, Peng et al. (Peng et al., 2005) developed a composite

membrane with a hydrophilic layer of polyvinyl alcohol (PVA) blended with polyethylene glycol (PEG) on a hydrophobic PVDF substrate for desalination. The composite membrane showed no wetting incident compared to hydrophobic membranes even after adding 25% ethanol to the brine feed. Later, Edwie et al. (Edwie and Chung, 2012) found out that membrane pore size and morphology beneath the membrane surface is more crucial to mitigate membrane wetting as compared to membrane wall thickness for a supersaturated NaCl feed solution. They fabricated three types of membranes including single-layer PVDF, dual-layer hydrophobic–hydrophobic PVDF and dual-layer hydrophobic–hydrophilic PVDF/polyacrylonitrile (PVDF/PAN) membranes. They found that the single-layer membrane possessing a smaller pore size and a cellular mixed-matrix structure outperformed the dual- layer membranes with a globular morphology with a superior wetting resistance. Triple layer nanofiber/hydrophobic/hydrophilic membranes have also been shown to increase in water CA and LEP. For this type of membranes (Fig. **16**), the intermediate hydrophobic layer increases the LEP of the membrane by narrowing the pore size, while the bottom surface-modifying macromolecules (hydrophilic) layer draws water vapor from the intermediate layer by absorption (Prince et al., 2014a).

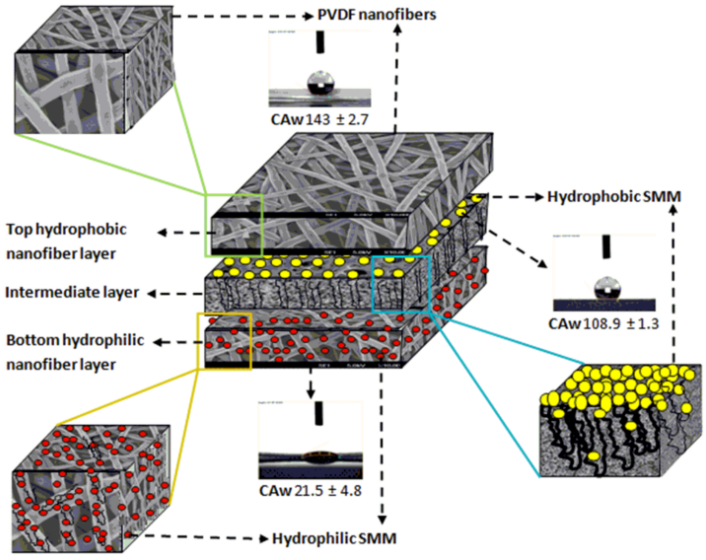

Fig. 16: The configuration of the triple layer membrane (Prince et al., 2014a).

Lin et al. (Lin et al., 2015) proposed a novel approach, hydrogel-covered membrane distillation (HcMD), by attaching an agarose hydrogel layer of a solid content of 6 wt.% with a thickness of 200 μm on the

surface of a PTFE membrane to reduce the risk of membrane wetting against various surfactants. The result showed no wetting during 24 h period when the concentration of surfactants was below critical micelle concentration (CMC) due to the repellency of hydrophobic moiety of the surfactant by the hydrogel phase. The agarose hydrogel with high water content acts as a static water layer by adsorbing the hydrophilic moiety and leaving the hydrophobic part outside of the surface, and preventing the surfactant from diffusing further into the hydrogel layer due to Donnan exclusion of ions (Bell, 2016) (Fig. **17a**). This causes the buildup of the surfactant molecules on the interface. Above the CMCs the wetting occurred due to diffusion of the absorbed hydrophilic moiety of micelles into the hydrogel phase, but to a lower extent and at a slower pace compared to bare membranes (Fig. **17b**). Attachment of hydrogel layer also decreased the permeate flux to about 71% of the flux using a bare membrane.

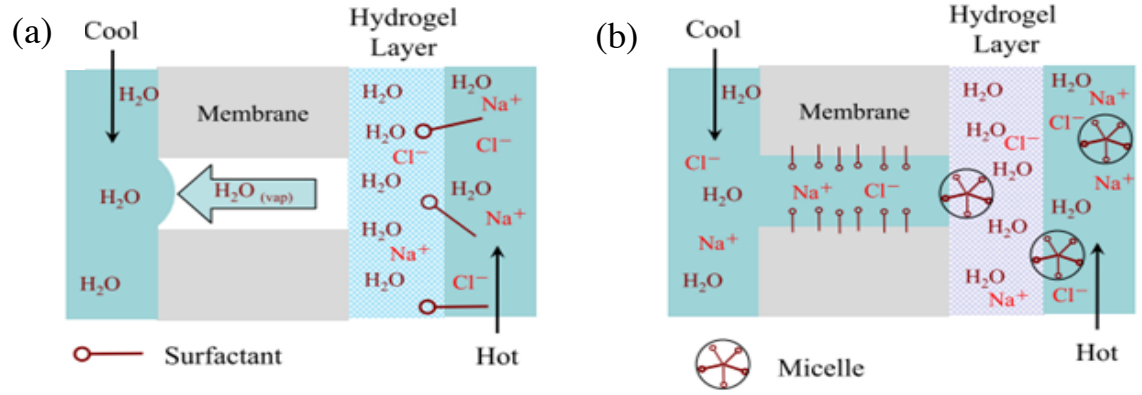

Fig. 17: The mechanism of hydrogel layer (a) against surfactant wetting (b) for the penetration of micelles through hydrogel layer.

12.3. Flow effects of buoyancy

Certain foulants have significant buoyancy differences from the bulk solution. MD systems can be designed to use this benefit to reduce surface adherence. For instance, in a study by Tan et al. (2017), inclined modules were used, with the membrane below the bulk fluid. The more buoyant oils in the seawater floated to the surface, and thus the inclination angle reduced fouling. This design works for flat plate modules (Warsinger et al., 2014), but the curved modules seen in the spiral wound and hollow fiber systems may be

759 more complex, as there will always be a surface above the foulant unless these modules are vertical (Tan
760 et al., 2017).

761 **12.4. Operating conditions**

762 Flow operating conditions can be chosen to avoid fouling. Such systems can use saturation
763 conditions, biocidal flow conditions, flow rates, and temperatures to minimize fouling. Past studies
764 have developed a framework for operating MD systems at supersaturated salinities of inorganic foulants,
765 by designing module geometry and saturation conditions so that the maximum residence time of potential
766 salt particles is less than the nucleation induction time (Warsinger et al., 2017b). This control of timescales
767 can inhibit inorganic deposition on the membrane, a major cause of wetting. Additionally, numerous studies
768 have shown that temperatures in excess of ~60°C have biocidal effects in desalination systems. Operating
769 conditions for avoiding wetting heavily overlap with conditions for preventing membrane fouling (D. M.
770 Warsinger et al., 2015).

771 **12.5. Membrane surface barrier protection**

772 Partial or complete removal of dissolved air from the feed water before MD causes a decrease in partial
773 pressure of air in the membrane due to equilibrium considerations. This is proved to lead to an increase in
774 pressure difference across the liquid/gas interface, thus increasing the tendency for membrane wetting (R
775 W Schofield et al., 1990). The use of gas bubbling has been considered for scaling and fouling control in
776 MD (Chen et al., 2014b, 2013; Ding et al., 2011). These studies have shown bubbling of air in the MD feed
777 could control fouling due to the reduced concentration polarization by increased mixing. Recently, a new
778 approach to control membrane wetting has been studied for MD systems by preventing adsorption
779 equilibrium at the liquid/solid interface through displacing the liquid which partly tends to penetrate the
780 macroporous membrane structure with gas bubbles (D. M. Warsinger et al., 2016; Rezaei et al., 2017b;
781 Rezaei and Samhaber, 2017a, 2017b). Therefore, based on the surface renewal theory (Danckwerts, 1951),
782 the wetting agents do not have enough time to accumulate on the macroporous structures, because the
783 interface is displaced or swept from the system by the gas bubbles. Recently, Rezaei et al. (Rezaei et al.,

2017a) examined the effect of recharging air bubbles on the membrane surfaces for the wetting incidence in a DCMD setup when a surfactant (sodium dodecyl sulfate, SDS) exists in a concentrated NaCl aqueous solution. The results showed that the in-situ air bubbles on the surface of the superhydrophobic membrane prevented the incident of wetting (~100% salt rejection) even for high concentrations of the surface-active species (up to 0.8mM SDS) in the feed solution. They concluded that introducing air into the feed side of the membrane displaces the liquid which partly tends to penetrate the macroporous structure with air bubbles and thus enhances the LEP, and also, the simultaneous use of a superhydrophobic membrane increases the solution CA (Fig. **18**). In the other studies (Chen et al., 2014c, 2013; Wu et al., 2015), the air bubbling in MD has also shown to improve the permeate flux due to the reduction of boundary layer effects and enhancement of heat and mass transfer. Therefore, the research on air bubbling in MD should be a future focus and its capability to achieve multiple improvements needs to be further investigated.

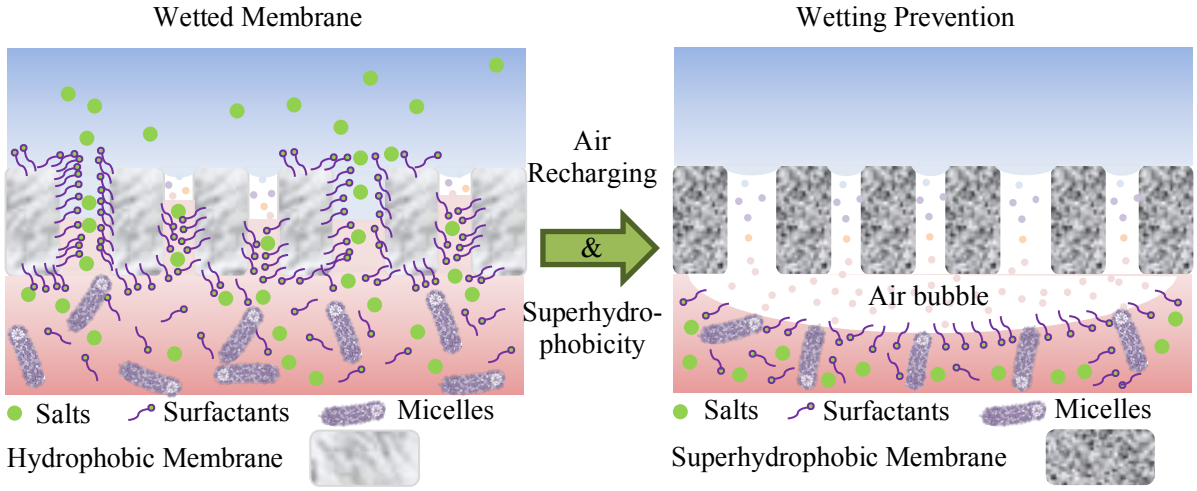

Fig. 18: Wetting prevention mechanism by maintaining an air layer on the surface of a superhydrophobic membrane (Rezaei et al., 2017a).

13. Conclusions and perspective

Wetting is a key challenge limiting the application of MD into a wider number of industrial applications. In such cases where wetting is a risk, membrane design and prevention methods have been shown to be effective in controlling wetting. Three degrees of wetting have been recognized in MD: surface wetting, partial wetting, and full wetting. Surface wetting is considered to lead to scaling as a result of solvent

evaporation inside the membrane pores but does not deteriorate permeate quality. Partial wetting takes place when solutions penetrate deeper into the larger pores leading to reduced permeate quality, while full wetting can incapacitate the process of MD.The literature shows that inorganic scaling and organic fouling are the main causes of membrane wetting, and different prevention methods are discussed. Several pretreatment processes are found to inhibit membrane wetting by removing the wetting agents from the feed solution. Various advanced membrane designs are evaluated to bring the surface non-wettability to the states of superhydrophobicity and superomniphobicity through altering not only the surface chemistry and surface geometrical structure, but also modifying the membrane wall properties. In summary, the following needs are proposed for further assessment of wetting phenomenon in MD.

- The possibility ofwetting occurrence for long-term performance and large-scale plant operations of MD needs to be further studied to obtain an entire outlook of the applicability of MD process for the treatment of solutions with low surface tension. When wetting has occurred, the possibility of its prevention should be investigated.
- Commercial hydrophobic membranes still suffer wetting due to capillary condensation. Therefore, development of a straight- forward and efficient approach for the fabrication of super-hydrophobic and superoleophobic surface for MD process is highly needed (Chew et al., 2017b; Z. Wang et al., 2017).
- Despite the promising prospect of MD with omniphobic mem- branes, additional investigations are required to examine other fabrication techniques and to optimize membrane performance. It is also crucial to assess the omniphobic membrane with a broad spectrum of surface-active agents and with feeds of more complex organic compositions (Liu (H. Liu et al., 2017).
- Potentially dangerous additives such as fluorinated chemicals are regarded as the persistent and global contaminants. New non-chemical methods such as pretreatment methods or other physical water treatment techniques to prevent wetting are should be evaluated.
- The impact of salinity and different organic foulants on the stability of the membrane with special wettability requires systematic research. Application of MD for the treatment of oily wastewater

with all main components should be more deeply studied, and more insight of the interaction between these elements via molecular dynamics simulations would be essential (Han et al., 2017).

- Further research is needed on the impact of air backwashing and air layer recharging for preventing fouling and wetting incidence in MD, especially at pilot scale.
- Due to lack of an appropriate model, mathematical models describing physics and thermodynamics of wetting phenomena for different wetting stages (i.e., surface, partial and full wetting) in MD need to be developed. To do so, a better mechanistic understanding of wetting as caused by different foulants is required
- More studies need to be focused on the design of large-scale MD modules, as regards the impact of module design on wetting and wetting reversal.
- Studies on improving membrane lifetime while avoiding wet- ting need to be conducted, and novel membrane material scale- up and testing for wetting should be established.

Funding

This research did not receive any specific grant from funding agencies in the public, commercial, or not-for-profit sectors.

Author Contributions

All authors have given approval to the final version of the manuscript.

Notes

The authors declare no competing financial interest.

Declarations of interest:

None.

Nomenclature

BSA	Bovine serum albumin
CA	Contact angle

CMC	Critical micelle concentration
DCMD	Direct contact membrane distillation
GF	Glass fiber
HA	Humic acid
HcMD	Hydrogel-covered membrane distillation
HLB	Hydrophilic-lipophilic balance
LEP	Liquid entry pressure
LTH	Low temperature hydrothermal
MD	Membrane distillation
NTIPS	Non-solvent thermally induced phase separation
PAB	Pressurized air backwashing
PP	Polypropylene
RO	Reverse osmosis
SEM	Scanning electron microscopy
VMD	Vacuum membrane distillation
WCA	Water contact angle

References

Adamson, A.W., Gast, A.P., 1997. Physical Chemistry of Surfaces, 6th ed. John Wiley & Sons, Ltd.

Ahmed, F.E., Lalia, B.S., Hashaikeh, R., 2017. Membrane-based detection of wetting phenomenon in direct contact membrane distillation. J. Memb. Sci. 535, 89–93. https://doi.org/10.1016/j.memsci.2017.04.035

Ali, M.I., Summers, E.K., Arafat, H.A., Lienhard, J.H., 2012. Effects of membrane properties on water production cost in small scale membrane distillation systems. Desalination 306, 60–71. https://doi.org/10.1016/j.desal.2012.07.043

877 Alkhudhiri, A., Darwish, N., Hilal, N., 2012. Membrane distillation: A comprehensive review. Desalination
878 287, 2–18. https://doi.org/10.1016/j.desal.2011.08.027
879 Alklaibi, A.M., Lior, N., 2005. Membrane-distillation desalination: Status and potential. Desalination 171,
880 111–131. https://doi.org/10.1016/j.desal.2004.03.024
881 An, A.K., Guo, J., Jeong, S., Lee, E.-J., Tabatabai, S.A.A., Leiknes, T., 2016a. High flux and antifouling
882 properties of negatively charged membrane for dyeing wastewater treatment by membrane distillation.
883 Water Res. 103, 362–371. https://doi.org/10.1016/j.watres.2016.07.060
884 An, A.K., Guo, J., Lee, E.-J., Jeong, S., Zhao, Y., Wang, Z., Leiknes, T., 2016b. PDMS/PVDF hybrid
885 electrospun membrane with superhydrophobic property and drop impact dynamics for dyeing
886 wastewater treatment using membrane distillation. J. Memb. Sci. 525, 57–67.
887 https://doi.org/10.1016/j.memsci.2016.10.028
888 An, S., Joshi, B.N., Lee, J.-G., Lee, M.W., Kim, Y. Il, Kim, M., Jo, H.S., Yoon, S.S., 2017. A
889 comprehensive review on wettability, desalination, and purification using graphene-based materials
890 at water interfaces. Catal. Today 295, 14–25. https://doi.org/10.1016/j.cattod.2017.04.027
891 Arafat, H., Bilad, M., Marzooqi, F., 2015. New Concept for Dual-Layer Hydrophilic/Hydrophobic
892 Composite Membrane for Membrane Distillation. J. Membr. Sep. Technol. 4, 122–133.
893 https://doi.org/10.6000/1929-6037.2015.04.03.4
894 Ashoor, B.B., Mansour, S., Giwa, A., Dufour, V., Hasan, S.W., 2016. Principles and applications of direct
895 contact membrane distillation (DCMD): A comprehensive review. Desalination 398, 222–246.
896 https://doi.org/10.1016/j.desal.2016.07.043
897 ASTM International, 2014. Standard Test Methods for Pore Size Characteristics of Membrane Filters by
898 Bubble Point and Mean Flow Pore Test. Astm 3, 1–7. https://doi.org/10.1520/F0316-03R11.2
899 Atchariyawut, S., Feng, C., Wang, R., Jiraratananon, R., Liang, D.T., 2006. Effect of membrane structure
900 on mass-transfer in the membrane gas-liquid contacting process using microporous PVDF hollow
901 fibers. J. Memb. Sci. 285, 272–281. https://doi.org/10.1016/j.memsci.2006.08.029
902 Babalou, A.A., Rafia, N., Ghasemzadeh, K., 2015. Pervaporation, Vapour Permeation and Membrane

903 Distillation, Pervaporation, Vapour Permeation and Membrane Distillation.
904 https://doi.org/10.1016/B978-1-78242-246-4.00003-9
905 Baghbanzadeh, M., Rana, D., Lan, C.Q., Matsuura, T., 2015. Effects of hydrophilic silica nanoparticles and
906 backing material in improving the structure and performance of VMD PVDF membranes. Sep. Purif.
907 Technol. 157, 60–71. https://doi.org/10.1016/j.seppur.2015.11.029
908 Bailey, A.F.G., Barbe, A.M., Hogan, P.A., Johnson, R.A., Sheng, J., 2000. The effect of ultrafiltration on
909 the subsequent concentration of grape juice by osmotic distillation. J. Memb. Sci. 164, 195–204.
910 https://doi.org/10.1016/S0376-7388(99)00209-4
911 Banat, F.A., Simandl, J., 1999. Membrane distillation for dilute ethanol. J. Memb. Sci. 163, 333–348.
912 https://doi.org/10.1016/S0376-7388(99)00178-7
913 Banat, F.A., Simandl, J., 1998. Desalination by Membrane Distillation: A Parametric Study. Sep. Sci.
914 Technol. 33, 201–226. https://doi.org/10.1080/01496399808544764
915 Banat, F.A., Simandl, J., 1994. Theoretical and experimental study in membrane distillation. Desalination
916 95, 39–52. https://doi.org/10.1016/0011-9164(94)00005-0
917 Barbe, A.M., Hogan, P.A., Johnson, R.A., 2000. Surface morphology changes during initial usage of
918 hydrophobic, microporous polypropylene membranes. J. Memb. Sci. 172, 149–156.
919 https://doi.org/10.1016/S0376-7388(00)00338-0
920 Bell, C.M., 2016. Comparison of polyelectrolyte coated PVDF membranes in thermopervaporation with
921 porous hydrophobic membranes in membrane distillation using plate-and-frame modules. Chem. Eng.
922 Process. Process Intensif. 104, 58–65. https://doi.org/10.1016/j.cep.2016.02.013
923 Bilad, M.R., Guillen-Burrieza, E., Mavukkandy, M.O., Al Marzooqi, F.A., Arafat, H.A., 2015. Shrinkage,
924 defect and membrane distillation performance of composite PVDF membranes. Desalination 376, 62–
925 72. https://doi.org/10.1016/j.desal.2015.08.015
926 Bodell, B.R., 1963. Silicone rubber vapor diffusion in saline water distillation. United States Pat. Ser.
927 Bonyadi, S., Chung, T.S., 2007. Flux enhancement in membrane distillation by fabrication of dual layer
928 hydrophilic-hydrophobic hollow fiber membranes. J. Memb. Sci. 306, 134–146.

https://doi.org/10.1016/j.memsci.2007.08.034

Boo, C., Lee, J., Elimelech, M., 2016. Engineering Surface Energy and Nanostructure of Microporous Films for Expanded Membrane Distillation Applications. Environ. Sci. Technol. 50, 8112–8119. https://doi.org/10.1021/acs.est.6b02316

Bouchrit, R., Boubakri, A., Hafiane, A., Bouguecha, S.A.T., 2015. Direct contact membrane distillation: Capability to treat hyper-saline solution. Desalination 376, 117–129. https://doi.org/10.1016/j.desal.2015.08.014

Brown, P.S., Bhushan, B., 2016. Designing bioinspired superoleophobic surfaces. APL Mater. 4. https://doi.org/10.1063/1.4935126

Camacho, L., Dumée, L., Zhang, J., Li, J., Duke, M., Gomez, J., Gray, S., 2013. Advances in Membrane Distillation for Water Desalination and Purification Applications. Water 5, 94–196. https://doi.org/10.3390/w5010094

Cao, L., Jones, A.K., Sikka, V.K., Wu, J., Gao, D., 2009. Anti-Icing Superhydrophobic Coatings 25, 12444–12448. https://doi.org/10.1021/la902882b

Carrero-Parreño, A., Onishi, V.C., Ruiz-Femenia, R., Salcedo-Díaz, R., Caballero, J.A., Reyes-Labarta, J.A., 2017. Multistage Membrane Distillation for the Treatment of Shale Gas Flowback Water: Multi-Objective Optimization under Uncertainty. Comput. Aided Chem. Eng. 40, 571–576. https://doi.org/10.1016/B978-0-444-63965-3.50097-0

Cassie, A.B.D., Baxter, S., 1944. Wettability of porous surfaces. Trans. Faraday Soc. 40, 546. https://doi.org/10.1039/tf9444000546

Cerneaux, S., Struzyńska, I., Kujawski, W.M., Persin, M., Larbot, A., 2009. Comparison of various membrane distillation methods for desalination using hydrophobic ceramic membranes. J. Memb. Sci. 337, 55–60. https://doi.org/10.1016/j.memsci.2009.03.025

Chanachai, A., Meksup, K., Jiraratananon, R., 2010. Coating of hydrophobic hollow fiber PVDF membrane with chitosan for protection against wetting and flavor loss in osmotic distillation process. Sep. Purif. Technol. 72, 217–224. https://doi.org/10.1016/j.seppur.2010.02.014

955 Chen, G., Lu, Y., Krantz, W.B., Wang, R., Fane, A.G., 2014a. Optimization of operating conditions for a
956 continuous membrane distillation crystallization process with zero salty water discharge. J. Memb.
957 Sci. 450, 1–11. https://doi.org/10.1016/j.memsci.2013.08.034
958 Chen, G., Yang, X., Lu, Y., Wang, R., Fane, A.G., 2014b. Heat transfer intensification and scaling
959 mitigation in bubbling-enhanced membrane distillation for brine concentration. J. Memb. Sci. 470,
960 60–69. https://doi.org/10.1016/j.memsci.2014.07.017
961 Chen, G., Yang, X., Lu, Y., Wang, R., Fane, A.G., 2014c. Heat transfer intensification and scaling
962 mitigation in bubbling-enhanced membrane distillation for brine concentration. J. Memb. Sci. 470,
963 60–69. https://doi.org/10.1016/j.memsci.2014.07.017
964 Chen, G., Yang, X., Wang, R., Fane, A.G., 2013. Performance enhancement and scaling control with gas
965 bubbling in direct contact membrane distillation. Desalination 308, 47–55.
966 https://doi.org/10.1016/j.desal.2012.07.018
967 Chen, K., Xiao, C., Huang, Q., Liu, H., Liu, H., Wu, Y., Liu, Z., 2015. Study on vacuum membrane
968 distillation (VMD) using FEP hollow fiber membrane. Desalination 375, 24–32.
969 https://doi.org/10.1016/j.desal.2015.07.021
970 Cheng, D.Y., Wiersma, S.J., 1983. Apparatus and method for thermal membrane distillation. US Parent
971 No. 4,419, 187.
972 Cheng, D.Y., Wiersma, S.J., 1983. Composite membrane for membrane distillation system. US4316772.
973 Cheng, T.-W., Han, C.-J., Hwang, K.-J., Ho, C.-D., Cooper, W.J., 2010. Influence of Feed Composition on
974 Distillate Flux and Membrane Fouling in Direct Contact Membrane Distillation. Sep. Sci. Technol.
975 45, 967–974. https://doi.org/10.1080/01496391003666908
976 Chew, J.W., Krantz, W.B., Fane, A.G., 2014. Effect of a macromolecular- or bio-fouling layer on
977 membrane distillation. J. Memb. Sci. 456, 66–76. https://doi.org/10.1016/j.memsci.2014.01.025
978 Chew, N.G.P., Zhao, S., Loh, C.H., Permogorov, N., Wang, R., 2017a. Surfactant effects on water recovery
979 from produced water via direct-contact membrane distillation. J. Memb. Sci. 528, 126–134.
980 https://doi.org/10.1016/j.memsci.2017.01.024

Chew, N.G.P., Zhao, S., Malde, C., Wang, R., 2017b. Superoleophobic surface modification for robust membrane distillation performance. J. Memb. Sci. 541, 162–173. https://doi.org/10.1016/j.memsci.2017.06.089

Chibowski, E., Terpilowski, K., 2008. Surface free energy of sulfur-Revisited. I. Yellow and orange samples solidified against glass surface. J. Colloid Interface Sci. 319, 505–513. https://doi.org/10.1016/j.jcis.2007.10.059

Cho, D.-W., Song, H., Yoon, K., Kim, S., Han, J., Cho, J., 2016. Treatment of Simulated Coalbed Methane Produced Water Using Direct Contact Membrane Distillation. Water 8, 194. https://doi.org/10.3390/w8050194

Choi, Y., Naidu, G., Jeong, S., Vigneswaran, S., Lee, S., Wang, R., Fane, A.G., 2017. Experimental comparison of submerged membrane distillation configurations for concentrated brine treatment. Desalination 420, 54–62. https://doi.org/10.1016/j.desal.2017.06.024

Chong, K.C., Lai, S.O., Thiam, H.S., Lee, S.S., Lau, W.J., Mokhtar, N.M., 2016. Reactive Blue Dye Removal by Membrane Distillation using PVDF Membrane. Indian J. Sci. Technol. 9, 1–5. https://doi.org/10.17485/ijst/2016/v9iS1/110379

Chua, Y.T., Ji, G., Birkett, G., Lin, C.X.C., Kleitz, F., Smart, S., 2015. Nanoporous organosilica membrane for water desalination: Theoretical study on the water transport. J. Memb. Sci. 482, 56–66. https://doi.org/10.1016/j.memsci.2015.01.060

Chul Woo, Y., Chen, Y., Tijing, L.D., Phuntsho, S., He, T., Choi, J.-S., Kim, S.-H., Kyong Shon, H., 2017. CF4 plasma-modified omniphobic electrospun nanofiber membrane for produced water brine treatment by membrane distillation. J. Memb. Sci. 529, 234–242. https://doi.org/10.1016/j.memsci.2017.01.063

Chung, H.W., Swaminathan, J., Warsinger, D.M., Lienhard, J.H., 2016. Multistage vacuum membrane distillation (MSVMD) systems for high salinity applications. J. Memb. Sci. 497, 128–141. https://doi.org/10.1016/j.memsci.2015.09.009

Courel, M., Dornier, M., Rios, G.M., Reynes, M., 2000. Modelling of water transport in osmotic distillation

using asymmetric membrane. J. Memb. Sci. 173, 107–122. https://doi.org/10.1016/S0376-7388(00)00348-3

Courel, M., Tronel-Peyroz, E., Rios, G.M., Dornier, M., Reynes, M., 2001. The problem of membrane characterization for the process of osmotic distillation. Desalination 140, 15–25. https://doi.org/10.1016/S0011-9164(01)00351-4

D. M. Warsinger, Swaminathan, A. Servi, J., V, J.H.L., 2016. Maintenance of gas layers for fouling prevention on submerged surfaces. 15/157,663.

Danckwerts, P. V., 1951. Significance of Liquid-Film Coefficients in Gas Absorption. Ind. Eng. Chem. 43, 1460–1467. https://doi.org/10.1021/ie50498a055

Darmanin, T., Guittard, F., 2013. Superoleophobic surfaces with short fluorinated chains? Soft Matter 9, 5982. https://doi.org/10.1039/c3sm50643f

Ding, Z., Liu, L., Liu, Z., Ma, R., 2011. The use of intermittent gas bubbling to control membrane fouling in concentrating TCM extract by membrane distillation. J. Memb. Sci. 372, 172–181. https://doi.org/10.1016/j.memsci.2011.01.063

Ding, Z., Liu, L., Liu, Z., Ma, R., 2010. Fouling resistance in concentrating TCM extract by direct contact membrane distillation. J. Memb. Sci. 362, 317–325. https://doi.org/10.1016/j.memsci.2010.06.040

Domingues, E., Arunachalam, S., Mishra, H., 2017. Doubly Reentrant Cavities Prevent Catastrophic Wetting Transitions on Intrinsically Wetting Surfaces. ACS Appl. Mater. Interfaces acsami.7b03526. https://doi.org/10.1021/acsami.7b03526

Dong, G., Kim, J.F., Kim, J.H., Drioli, E., Lee, Y.M., 2017. Open-source predictive simulators for scale-up of direct contact membrane distillation modules for seawater desalination. Desalination 402, 72–87. https://doi.org/10.1016/j.desal.2016.08.025

Dong, Z.-Q., Ma, X.-H., Xu, Z.-L., Gu, Z.-Y., 2015. Superhydrophobic modification of PVDF/SiO2 electrospun nanofiber membranes for vacuum membrane distillation. RSC Adv. 5, 67962–67970. https://doi.org/10.1039/C5RA10575G

Dong, Z.-Q.Q., Wang, B.-J.J., Ma, X.H., Wei, Y.-M.M., Xu, Z.-L.L., 2015. FAS Grafted Electrospun

Poly(vinyl alcohol) Nanofiber Membranes with Robust Superhydrophobicity for Membrane Distillation. ACS Appl. Mater. Interfaces 7, 22652–22659. https://doi.org/10.1021/acsami.5b07454

Dong, Z.Q., Ma, X. hua, Xu, Z.L., You, W.T., Li, F. bing, 2014. Superhydrophobic PVDF-PTFE electrospun nanofibrous membranes for desalination by vacuum membrane distillation. Desalination 347, 175–183. https://doi.org/10.1016/j.desal.2014.05.015

Dow, N., Villalobos García, J., Naidoo, L., Milne, N., Zhang, J., Gray, S., Duke, M., 2017. Demonstration of membrane distillation on textile waste water: assessment of long term performance, membrane cleaning and waste heat integration. Environ. Sci. Water Res. Technol. https://doi.org/10.1039/C6EW00290K

Dumée, L.F., Alglave, H., Chaffraix, T., Lin, B., Magniez, K., Schütz, J., 2016. Morphology-properties relationship of gas plasma treated hydrophobic meso-porous membranes and their improved performance for desalination by membrane distillation. Appl. Surf. Sci. 363, 273–285. https://doi.org/10.1016/j.apsusc.2015.12.034

Dumée, L.F., Gray, S., Duke, M., Sears, K., Schütz, J., Finn, N., 2013. The role of membrane surface energy on direct contact membrane distillation performance. Desalination 323, 22–30. https://doi.org/10.1016/j.desal.2012.07.012

Durham, R.J., Nguyen, M.H., 1994. Hydrophobic membrane evaluation and cleaning for osmotic distillation of tomato puree. J. Memb. Sci. 87, 181–189. https://doi.org/10.1016/0376-7388(93)E0142-7

Edwie, F., Chung, T.S., 2013. Development of simultaneous membrane distillation-crystallization (SMDC) technology for treatment of saturated brine. Chem. Eng. Sci. 98, 160–172. https://doi.org/10.1016/j.ces.2013.05.008

Edwie, F., Chung, T.S., 2012. Development of hollow fiber membranes for water and salt recovery from highly concentrated brine via direct contact membrane distillation and crystallization. J. Memb. Sci. 421–422, 111–123. https://doi.org/10.1016/j.memsci.2012.07.001

Edwie, F., Teoh, M.M., Chung, T.-S., 2012. Effects of additives on dual-layer hydrophobic–hydrophilic

PVDF hollow fiber membranes for membrane distillation and continuous performance. Chem. Eng. Sci. 68, 567–578. https://doi.org/10.1016/j.ces.2011.10.024

Efome, J.E., Rana, D., Matsuura, T., Lan, C.Q., 2016. Enhanced performance of PVDF nanocomposite membrane by nanofiber coating: A membrane for sustainable desalination through MD. Water Res. 89, 39–49. https://doi.org/10.1016/j.watres.2015.11.040

El-Abbassi, A., Hafidi, A., Khayet, M., García-Payo, M.C., 2013. Integrated direct contact membrane distillation for olive mill wastewater treatment. Desalination 323, 31–38. https://doi.org/10.1016/j.desal.2012.06.014

El-Bourawi, M.S., Ding, Z., Ma, R., Khayet, M., 2006. A framework for better understanding membrane distillation separation process. J. Memb. Sci. 285, 4–29. https://doi.org/10.1016/j.memsci.2006.08.002

Eykens, L., De Sitter, K., Dotremont, C., De Schepper, W., Pinoy, L., Van Der Bruggen, B., 2017. Wetting Resistance of Commercial Membrane Distillation Membranes in Waste Streams Containing Surfactants and Oil. Appl. Sci. 7, 118. https://doi.org/10.3390/app7020118

Eykens, L., De Sitter, K., Dotremont, C., Pinoy, L., Van der Bruggen, B., 2017. Membrane synthesis for membrane distillation: A review. Sep. Purif. Technol. https://doi.org/10.1016/j.seppur.2017.03.035

Eykens, L., De Sitter, K., Dotremont, C., Pinoy, L., Van Der Bruggen, B., 2016. How to Optimize the Membrane Properties for Membrane Distillation: A Review. Ind. Eng. Chem. Res. 55, 9333–9343. https://doi.org/10.1021/acs.iecr.6b02226

Fan, X., Liu, Y., Quan, X., Zhao, H., Chen, S., Yi, G., Du, L., 2016. High desalination permeability, wetting and fouling resistance on superhydrophobic carbon nanotube hollow fiber membrane under self-powered electrochemical assistance. J. Memb. Sci. 514, 501–509. https://doi.org/10.1016/j.memsci.2016.05.003

Fan, Y., Chen, S., Zhao, H., Liu, Y., 2017. Distillation membrane constructed by TiO2 nanofiber followed by fluorination for excellent water desalination performance. Desalination 405, 51–58. https://doi.org/10.1016/j.desal.2016.11.028

1085 Fane, A.G., Wang, R., Tang, C.Y., Yang, X., 2012. Membrane distillation and forward osmosis: advances
1086 in membranes, modules, and applications. IDA J. 4, 22–26.
1087 Feng, B.X., Jiang, L., 2006. Design and Creation of Superwetting / Antiwetting Surfaces 3063–3078.
1088 https://doi.org/10.1002/adma.200501961
1089 Feng, X., Jiang, L.Y., Matsuura, T., Wu, P., 2017. Fabrication of hydrophobic/hydrophilic composite
1090 hollow fibers for DCMD: Influence of dope formulation and external coagulant. Desalination 401,
1091 53–63. https://doi.org/10.1016/j.desal.2016.07.026
1092 Feng, X., Jiang, L.Y., Song, Y., 2016. Titanium white sulfuric acid concentration by direct contact
1093 membrane distillation. Chem. Eng. J. 285, 101–111. https://doi.org/10.1016/j.cej.2015.09.064
1094 Figoli, A., Ursino, C., Galiano, F., Di Nicolò, E., Carnevale, M.C., Criscuoli, A., 2016. Innovative
1095 hydrophobic coating of perfluoropolyether (PFPE) on commercial hydrophilic membranes for DCMD
1096 application. J. Memb. Sci. https://doi.org/10.1016/j.memsci.2016.08.066
1097 Franco, J.A., Kentish, S.E., Perera, J.M., Stevens, G.W., 2008. Fabrication of a superhydrophobic
1098 polypropylene membrane by deposition of a porous crystalline polypropylene coating. J. Memb. Sci.
1099 318, 107–113. https://doi.org/10.1016/j.memsci.2008.02.032
1100 Franken, A.C.M., Nolten, J.A.M., Mulder, M.H.V., Bargeman, D., Smolders, C.A., 1987. Wetting criteria
1101 for the applicability of membrane distillation. J. Memb. Sci. 33, 315–328.
1102 https://doi.org/10.1016/S0376-7388(00)80288-4
1103 García-Fernández, L., García-Payo, M.C., Khayet, M., 2014. Effects of mixed solvents on the structural
1104 morphology and membrane distillation performance of PVDF-HFP hollow fiber membranes. J.
1105 Memb. Sci. 468, 324–338. https://doi.org/10.1016/j.memsci.2014.06.014
1106 García-Payo, M.C., Izquierdo-Gil, M.A., Fernández-Pineda, C., 2000. Wetting Study of Hydrophobic
1107 Membranes via Liquid Entry Pressure Measurements with Aqueous Alcohol Solutions. J. Colloid
1108 Interface Sci. 230, 420–431. https://doi.org/10.1006/jcis.2000.7106
1109 Ge, J., Peng, Y., Li, Z., Chen, P., Wang, S., 2014. Membrane fouling and wetting in a DCMD process for
1110 RO brine concentration. Desalination 344, 97–107. https://doi.org/10.1016/j.desal.2014.03.017

1111 Gilron, J., Ladizansky, Y., Korin, E., 2013. Silica fouling in direct contact membrane distillation. Ind. Eng.
1112 Chem. Res. 52, 10521–10529. https://doi.org/10.1021/ie400265b
1113 Goh, S., Zhang, J., Liu, Y., Fane, A.G., 2013. Fouling and wetting in membrane distillation (MD) and MD-
1114 bioreactor (MDBR) for wastewater reclamation. Desalination 323, 39–47.
1115 https://doi.org/10.1016/j.desal.2012.12.001
1116 González-Benito, J., Teno, J., González-Gaitano, G., Xu, S., Chiang, M.Y., 2017. PVDF/TiO2
1117 nanocomposites prepared by solution blow spinning: Surface properties and their relation with
1118 S. Mutans adhesion. Polym. Test. 58, 21–30. https://doi.org/10.1016/j.polymertesting.2016.12.005
1119 Grynyov, R., Bormashenko, E., Whyman, G., Bormashenko, Y., Musin, A., Pogreb, R., Starostin, A.,
1120 Valtsifer, V., Strelnikov, V., Schechter, A., Kolagatla, S., 2016. Superoleophobic Surfaces Obtained
1121 via Hierarchical Metallic Meshes. Langmuir 32, 4134–4140.
1122 https://doi.org/10.1021/acs.langmuir.6b00248
1123 Gryta, M., 2017. The application of polypropylene membranes for production of fresh water from brines
1124 by membrane distillation. Chem. Pap. 71, 775–784. https://doi.org/10.1007/s11696-016-0059-6
1125 Gryta, M., 2016a. The Application of Membrane Distillation for Broth Separation in Membrane
1126 Bioreactors. J. Membr. Sci. Res. 2, 193–200.
1127 Gryta, M., 2016b. The study of performance of polyethylene chlorinetrifluoroethylene membranes used for
1128 brine desalination by membrane distillation. Desalination 398, 52–63.
1129 https://doi.org/10.1016/j.desal.2016.07.021
1130 Gryta, M., 2015. Water desalination using membrane distillation with acidic stabilization of scaling layer
1131 thickness. Desalination 365, 160–166. https://doi.org/10.1016/j.desal.2015.02.031
1132 Gryta, M., 2008. Fouling in direct contact membrane distillation process. J. Memb. Sci. 325, 383–394.
1133 https://doi.org/10.1016/j.memsci.2008.08.001
1134 Gryta, M., 2007a. Influence of polypropylene membrane surface porosity on the performance of membrane
1135 distillation process. J. Memb. Sci. 287, 67–78. https://doi.org/10.1016/j.memsci.2006.10.011
1136 Gryta, M., 2007b. Effect of iron oxides scaling on the MD process performance. Desalination 216, 88–102.

https://doi.org/10.1016/j.desal.2007.01.002

Gryta, M., 2005. Long-term performance of membrane distillation process. J. Memb. Sci. 265, 153–159. https://doi.org/10.1016/j.memsci.2005.04.049

Gryta, M., 2002. Direct contact membrane distillation with crystallization applied to NaCl solutions. Chem. Pap. 56, 14–19.

Gryta, M., 2002a. The assessment of microorganism growth in the membrane distillation system. Desalination 142, 79–88. https://doi.org/10.1016/S0011-9164(01)00427-1

Gryta, M., 2002b. Concentration of NaCl solution by membrane distillation integrated with crystallization. Sep. Sci. Technol. 37, 3535–3558. https://doi.org/10.1081/SS-120014442

Gryta, M., Barancewicz, M., 2010. Influence of morphology of PVDF capillary membranes on the performance of direct contact membrane distillation. J. Memb. Sci. 358, 158–167. https://doi.org/10.1016/j.memsci.2010.04.044

Gryta, M., Grzechulska-Damszel, J., Markowska, A., Karakulski, K., 2009. The influence of polypropylene degradation on the membrane wettability during membrane distillation. J. Memb. Sci. 326, 493–502. https://doi.org/10.1016/j.memsci.2008.10.022

Gryta, M., Tomaszewska, M., Morawski, A.W., 1997. Membrane distillation with laminar flow. Sep. Purif. Technol. 11, 93–101. https://doi.org/10.1016/S1383-5866(97)00002-6

Guillén-Burrieza, E., Blanco, J., Zaragoza, G., Alarcón, D.-C., Palenzuela, P., Ibarra, M., Gernjak, W., 2011. Experimental analysis of an air gap membrane distillation solar desalination pilot system. J. Memb. Sci. 379, 386–396. https://doi.org/10.1016/j.memsci.2011.06.009

Guillen-Burrieza, E., Mavukkandy, M.O., Bilad, M.R., Arafat, H.A., 2016. Understanding wetting phenomena in membrane distillation and how operational parameters can affect it. J. Memb. Sci. 515, 163–174. https://doi.org/10.1016/j.memsci.2016.05.051

Guillen-Burrieza, E., Ruiz-Aguirre, A., Zaragoza, G., Arafat, H.A., 2014. Membrane fouling and cleaning in long term plant-scale membrane distillation operations. J. Memb. Sci. 468, 360–372. https://doi.org/10.1016/j.memsci.2014.05.064

1163 Guillen-Burrieza, E., Servi, A., Lalia, B.S., Arafat, H.A., 2015. Membrane structure and surface
1164 morphology impact on the wetting of MD membranes. J. Memb. Sci. 483, 94–103.
1165 https://doi.org/10.1016/j.memsci.2015.02.024
1166 Guillen-Burrieza, E., Thomas, R., Mansoor, B., Johnson, D., Hilal, N., Arafat, H., 2013. Effect of dry-out
1167 on the fouling of PVDF and PTFE membranes under conditions simulating intermittent seawater
1168 membrane distillation (SWMD). J. Memb. Sci. 438, 126–139.
1169 https://doi.org/10.1016/j.memsci.2013.03.014
1170 Guo, F., Servi, A., Liu, A., Gleason, K.K., Rutledge, G.C., 2015. Desalination by Membrane Distillation
1171 using Electrospun Polyamide Fiber Membranes with Surface Fluorination by Chemical Vapor
1172 Deposition. ACS Appl. Mater. Interfaces 7, 8225–8232. https://doi.org/10.1021/acsami.5b01197
1173 Hammami, M.A., Croissant, J., Francis, L., Alsaiari, S.K., Anjum, D.H., Ghaffour, N., Khashab, N.M.,
1174 2016. Engineering Hydrophobic Organosilica Doped Nanofibers for Enhanced and Fouling Resistant
1175 Membrane Distillation. ACS Appl. Mater. Interfaces acsami.6b11167.
1176 https://doi.org/10.1021/acsami.6b11167
1177 Hamzah, N., Leo, C.P., 2017. Membrane distillation of saline with phenolic compound using
1178 superhydrophobic PVDF membrane incorporated with TiO2 nanoparticles: Separation, fouling and
1179 self-cleaning evaluation. Desalination 418, 79–88. https://doi.org/10.1016/j.desal.2017.05.029
1180 Han, L., Tan, Y.Z., Netke, T., Fane, A.G., Chew, J.W., 2017. Understanding oily wastewater treatment via
1181 membrane distillation. J. Memb. Sci. 539, 284–294. https://doi.org/10.1016/j.memsci.2017.06.012
1182 Hassan, M.I., Brimmo, A.T., Swaminathan, J., Lienhard, J.H., Arafat, H.A., 2015. A new vacuum
1183 membrane distillation system using an aspirator: concept modeling and optimization. Desalin. Water
1184 Treat. 57, 12915–12928. https://doi.org/10.1080/19443994.2015.1060902
1185 Hausmann, A., Sanciolo, P., Vasiljevic, T., Ponnampalam, E., Quispe-Chavez, N., Weeks, M., Duke, M.,
1186 2011. Direct contact membrane distillation of dairy process streams. Membranes (Basel). 1, 48–58.
1187 https://doi.org/10.3390/membranes1010048
1188 He, F., Gilron, J., Lee, H., Song, L., Sirkar, K.K., 2008. Potential for scaling by sparingly soluble salts in

crossflow DCMD. J. Memb. Sci. 311, 68–80. https://doi.org/10.1016/j.memsci.2007.11.056

He, F., Sirkar, K.K., Gilron, J., 2009. Effects of antiscalants to mitigate membrane scaling by direct contact membrane distillation. J. Memb. Sci. 345, 53–58. https://doi.org/10.1016/j.memsci.2009.08.021

Hickenbottom, K.L., Cath, T.Y., 2014. Sustainable operation of membrane distillation for enhancement of mineral recovery from hypersaline solutions. J. Memb. Sci. 454, 426–435. https://doi.org/10.1016/j.memsci.2013.12.043

Hou, D., Lin, D., Zhao, C., Wang, J., Fu, C., 2017. Control of protein (BSA) fouling by ultrasonic irradiation during membrane distillation process. Sep. Purif. Technol. 175, 287–297. https://doi.org/10.1016/j.seppur.2016.11.047

Hou, D., Wang, Z., Li, G., Fan, H., Wang, J., Huang, H., 2015. Ultrasonic assisted direct contact membrane distillation hybrid process for membrane scaling mitigation. Desalination 375, 33–39. https://doi.org/10.1016/j.desal.2015.07.018

Huang, C.-Y., Ko, C.-C., Chen, L.-H., Huang, C.-T., Tung, K.-L., Liao, Y.-C., 2016. A simple coating method to prepare superhydrophobic layers on ceramic alumina for vacuum membrane distillation. Sep. Purif. Technol. https://doi.org/10.1016/j.seppur.2016.12.037

Huang, Y.-X., Wang, Z., Hou, D., Lin, S., 2017. Coaxially Electrospun Super-amphiphobic Silica-based Membrane for Anti-surfactant-wetting Membrane Distillation. J. Memb. Sci. https://doi.org/10.1016/j.memsci.2017.02.044

Husnain, T., Liu, Y., Riffat, R., Mi, B., 2015. Integration of forward osmosis and membrane distillation for sustainable wastewater reuse. Sep. Purif. Technol. 156, 424–431. https://doi.org/10.1016/j.seppur.2015.10.031

Jang, Y., Cho, H., Shin, Y., Choi, Y., Lee, S., Koo, J., 2016. Comparison of fouling propensity and physical cleaning effect in forward osmosis, reverse osmosis, and membrane distillation. Desalin. Water Treat. 57, 24532–24541. https://doi.org/10.1080/19443994.2016.1152650

Jeong, S., Lee, S., Chon, H.T., Lee, S., 2014. Structural analysis and modeling of the commercial high performance composite flat sheet membranes for membrane distillation application. Desalination 349,

115–125. https://doi.org/10.1016/j.desal.2014.05.027

Jin, Z., Yang, D.L., Zhang, S.H., Jian, X.G., 2008. Hydrophobic modification of poly(phthalazinone ether sulfone ketone) hollow fiber membrane for vacuum membrane distillation. Chinese Chem. Lett. 19, 367–370. https://doi.org/10.1016/j.cclet.2007.12.029

Joly, L., Biben, T., 2009. Wetting and friction on superoleophobic surfaces. Soft Matter. https://doi.org/10.1039/b821214g

Kang, G., Cao, Y., 2014. Application and modification of poly(vinylidene fluoride) (PVDF) membranes – A review. J. Memb. Sci. 463, 145–165. https://doi.org/10.1016/j.memsci.2014.03.055

Karakulski, K., Gryta, M., 2005. Water demineralisation by NF/MD integrated processes. Desalination 177, 109–119. https://doi.org/10.1016/j.desal.2004.11.018

Kayvani Fard, A., Rhadfi, T., Khraisheh, M., Atieh, M.A., Khraisheh, M., Hilal, N., 2016. Reducing flux decline and fouling of direct contact membrane distillation by utilizing thermal brine from MSF desalination plant. Desalination 379, 172–181. https://doi.org/10.1016/j.desal.2015.11.004

Keurentjes, J.T.F., Harbrecht, J.G., Brinkman, D., Hanemaaijer, J.H., Cohen Stuart, M.A., van't Riet, K., 1989. Hydrophobicity measurements of microfiltration and ultrafiltration membranes. J. Memb. Sci. 47, 333–344. https://doi.org/10.1016/S0376-7388(00)83084-7

Kezia, K., Lee, J., Weeks, M., Kentish, S., 2015. Direct contact membrane distillation for the concentration of saline dairy effluent. Water Res. 81, 167–177. https://doi.org/10.1016/j.watres.2015.05.042

Khayet, M., Matsuura, T., 2004. Pervaporation and vacuum membrane distillation processes: Modeling and experiments. AIChE J. 50, 1697–1712. https://doi.org/10.1002/aic.10161

Khemakhem, S., Amar, R. Ben, 2011. Grafting of fluoroalkylsilanes on microfiltration Tunisian clay membrane. Ceram. Int. 37, 3323–3328. https://doi.org/10.1016/j.ceramint.2011.04.128

Kim, J., Kwon, H., Lee, S.S., Lee, S.S., Hong, S., 2016. Membrane distillation (MD) integrated with crystallization (MDC) for shale gas produced water (SGPW) treatment. Desalination 403, 4–7. https://doi.org/10.1016/j.desal.2016.07.045

Kota, A.K., Mabry, J.M., Tuteja, A., 2013. Superoleophobic surfaces: design criteria and recent studies.

1241 Surf. Innov. 1, 71–83. https://doi.org/10.1680/si.12.00017
1242 Kota, A.K., Tuteja, A., 2012. Superoleophobic surfaces. ACS Symp. Ser. 1106, 171–185.
1243 https://doi.org/10.1021/bk-2012-1106.ch011
1244 Krivorot, M., Kushmaro, A., Oren, Y., Gilron, J., 2011. Factors affecting biofilm formation and biofouling
1245 in membrane distillation of seawater. J. Memb. Sci. 376, 15–24.
1246 https://doi.org/10.1016/j.memsci.2011.01.061
1247 Kujawa, J., Al-Gharabli, S., Kujawski, W., Knozowska, K., 2017. Molecular Grafting of Fluorinated and
1248 Nonfluorinated Alkylsiloxanes on Various Ceramic Membrane Surfaces for the Removal of Volatile
1249 Organic Compounds Applying Vacuum Membrane Distillation. ACS Appl. Mater. Interfaces 9,
1250 6571–6590. https://doi.org/10.1021/acsami.6b14835
1251 Kujawa, J., Cerneaux, S., Kujawski, W., Bryjak, M., Kujawski, J., 2016. How To Functionalize Ceramics
1252 by Perfluoroalkylsilanes for Membrane Separation Process? Properties and Application of
1253 Hydrophobized Ceramic Membranes. ACS Appl. Mater. Interfaces 8, 7564–77.
1254 https://doi.org/10.1021/acsami.6b00140
1255 Kujawa, J., Kujawski, W., 2016. Functionalization of Ceramic Metal Oxide Powders and Ceramic
1256 Membranes by Perfluroalkylsilanes and Alkylsilanes Possessing Different Reactive Groups –
1257 Physicochemical and Tribological Properties. ACS Appl. Mater. Interfaces acsami.5b11975.
1258 https://doi.org/10.1021/acsami.5b11975
1259 Kujawska, A., Kujawski, J.K., Bryjak, M., Cichosz, M., Kujawski, W., 2016. Removal of volatile organic
1260 compounds from aqueous solutions applying thermally driven membrane processes. 2. Air gap
1261 membrane distillation. J. Memb. Sci. 499, 245–256. https://doi.org/10.1016/j.memsci.2015.10.047
1262 Kujawski, W., Kujawa, J., Wierzbowska, E., Cerneaux, S., Bryjak, M., Kujawski, J., 2016. Influence of
1263 hydrophobization conditions and ceramic membranes pore size on their properties in vacuum
1264 membrane distillation of water-organic solvent mixtures. J. Memb. Sci. 499, 442–451.
1265 https://doi.org/10.1016/j.memsci.2015.10.067
1266 Kumar, R., Ghosh, A.K., Pal, P., 2017. Fermentative energy conversion: Renewable carbon source to

biofuels (ethanol) using Saccharomyces cerevisiae and downstream purification through solar driven membrane distillation and nanofiltration. Energy Convers. Manag. 150, 545–557. https://doi.org/10.1016/j.enconman.2017.08.054

Kwok, D.Y., Neumann, a. W., 1999. Contact angle measurement and contact angle interpretation, Advances in Colloid and Interface Science. https://doi.org/10.1016/S0001-8686(98)00087-6

Kyoungjin An, A., Lee, E.-J., Guo, J., Jeong, S., Lee, J.-G., Ghaffour, N., 2017. Enhanced vapor transport in membrane distillation via functionalized carbon nanotubes anchored into electrospun nanofibres. Sci. Rep. 7, 41562. https://doi.org/10.1038/srep41562

Lalia, B.S., Guillen-Burrieza, E., Arafat, H.A., Hashaikeh, R., 2013. Fabrication and characterization of polyvinylidenefluoride-co-hexafluoropropylene (PVDF-HFP) electrospun membranes for direct contact membrane distillation. J. Memb. Sci. 428, 104–115. https://doi.org/10.1016/j.memsci.2012.10.061

Lalia, B.S., Guillen, E., Arafat, H.A., Hashaikeh, R., 2014. Nanocrystalline cellulose reinforced PVDF-HFP membranes for membrane distillation application. Desalination 332, 134–141. https://doi.org/10.1016/j.desal.2013.10.030

Lawal, D.U., Khalifa, A.E., 2015. Experimental investigation of an air gap membrane distillation unit with double-sided cooling channel. Desalin. Water Treat. 1–15. https://doi.org/10.1080/19443994.2015.1042065

Lawson, K.W., Lloyd, D.R., 1997. Membrane distillation. J. Memb. Sci. 124, 1–25. https://doi.org/10.1016/S0376-7388(96)00236-0

Lee, E.-J., An, A.K., Hadi, P., Lee, S., Woo, Y.C., Shon, H.K., 2017. Advanced multi-nozzle electrospun functionalized titanium dioxide/polyvinylidene fluoride-co-hexafluoropropylene (TiO 2 /PVDF-HFP) composite membranes for direct contact membrane distillation. J. Memb. Sci. 524, 712–720. https://doi.org/10.1016/j.memsci.2016.11.069

Lee, E.-J.J., An, A.K., He, T., Woo, Y.C., Shon, H.K., 2016. Electrospun nanofiber membranes incorporating fluorosilane-coated TiO2 nanocomposite for direct contact membrane distillation. J.

Memb. Sci. 520, 145–154. https://doi.org/10.1016/j.memsci.2016.07.019

Lee, J.-G., Lee, E.-J., Jeong, S., Guo, J., An, A.K., Guo, H., Kim, J., Leiknes, T., Ghaffour, N., 2017. Theoretical modeling and experimental validation of transport and separation properties of carbon nanotube electrospun membrane distillation. J. Memb. Sci. 526, 395–408. https://doi.org/10.1016/j.memsci.2016.12.045

Lee, J., Boo, C., Ryu, W.-H., Taylor, A.D., Elimelech, M., 2016. Development of Omniphobic Desalination Membranes Using a Charged Electrospun Nanofiber Scaffold. ACS Appl. Mater. Interfaces 8, 11154–61. https://doi.org/10.1021/acsami.6b02419

Lee, J.G., Jang, Y., Fortunato, L., Jeong, S., Lee, S., Leiknes, T.O., Ghaffour, N., 2018. An advanced online monitoring approach to study the scaling behavior in direct contact membrane distillation. J. Memb. Sci. 546, 50–60. https://doi.org/10.1016/j.memsci.2017.10.009

Lee, J.G., Kim, Y.D., Kim, W.S., Francis, L., Amy, G., Ghaffour, N., 2015. Performance modeling of direct contact membrane distillation (DCMD) seawater desalination process using a commercial composite membrane. J. Memb. Sci. 478, 85–95. https://doi.org/10.1016/j.memsci.2014.12.053

Li, B., Sirkar, K.K., 2005. Novel membrane and device for vacuum membrane distillation-based desalination process. J. Memb. Sci. 257, 60–75. https://doi.org/10.1016/j.memsci.2004.08.040

Li, B., Sirkar, K.K., 2004. Novel Membrane and Device for Direct Contact Membrane Distillation-Based Desalination Process. Ind. Eng. Chem. Res. 43, 5300–5309. https://doi.org/10.1021/ie030871s

Li, J., Hou, D., Li, K., Zhang, Y., Wang, J., Zhang, X., 2018. Domestic wastewater treatment by forward osmosis-membrane distillation (FO-MD) integrated system. Water Sci. Technol. wst2018031. https://doi.org/10.2166/wst.2018.031

Li, L., Li, B., Dong, J., Zhang, J., 2016. Roles of silanes and silicones in forming superhydrophobic and superoleophobic materials. J. Mater. Chem. A 4, 13677–13725. https://doi.org/10.1039/C6TA05441B

Li, X., Deng, L., Yu, X., Wang, M., Wang, X., García-Payo, C., Khayet, M., 2016. A Novel Profiled Core-Shell Nanofibrous Membrane for Wastewater Treatment by Direct Contact Membrane Distillation. J. Mater. Chem. A. https://doi.org/10.1039/C6TA05492G

1319 Li, X., Wang, C., Yang, Y., Wang, X., Zhu, M., Hsiao, B.S., 2014a. Dual-Biomimetic Superhydrophobic
1320 Electrospun Polystyrene Nanofibrous Membranes for Membrane Distillation. ACS Appl. Mater.
1321 Interfaces 6, 2423–2430. https://doi.org//10.1021/am4048128
1322 Li, X., Wang, C., Yang, Y., Wang, X., Zhu, M., Hsiao, B.S., 2014b. Dual-Biomimetic Superhydrophobic
1323 Electrospun Polystyrene Nanofibrous Membranes for Membrane Distillation. ACS Appl. Mater.
1324 Interfaces 6, 2423–2430. https://doi.org/10.1021/am4048128
1325 Li, X., Yu, X., Cheng, C., Deng, L., Wang, M., Wang, X., 2015. Electrospun Superhydrophobic
1326 Organic/Inorganic Composite Nanofibrous Membranes for Membrane Distillation. ACS Appl. Mater.
1327 Interfaces 7, 21919–21930. https://doi.org/10.1021/acsami.5b06509
1328 Li, Y., Zhu, Z., Yu, J., Ding, B., 2015. Carbon Nanotubes Enhanced Fluorinated Polyurethane Macroporous
1329 Membranes for Waterproof and Breathable Application. ACS Appl. Mater. Interfaces 7, 13538–
1330 13546. https://doi.org/10.1021/acsami.5b02848
1331 Liao, Y., Wang, R., Fane, A.G., 2013. Engineering superhydrophobic surface on poly(vinylidene fluoride)
1332 nanofiber membranes for direct contact membrane distillation. J. Memb. Sci. 440, 77–87.
1333 https://doi.org/10.1016/j.memsci.2013.04.006
1334 Lin, P.-J., Yang, M.-C., Li, Y.-L., Chen, J.-H., 2015. Prevention of surfactant wetting with agarose hydrogel
1335 layer for direct contact membrane distillation used in dyeing wastewater treatment. J. Memb. Sci. 475,
1336 511–520. https://doi.org/10.1016/j.memsci.2014.11.001
1337 Lin, S., Nejati, S., Boo, C., Hu, Y., Osuji, C.O., Elimelech, M., 2014. Omniphobic Membrane for Robust
1338 Membrane Distillation. Environ. Sci. Technol. Lett. 1, 443–447. https://doi.org/10.1021/ez500267p
1339 Liu, C., Chen, L., Zhu, L., 2017. Fouling behavior of lysozyme on different membrane surfaces during the
1340 MD operation: An especial interest in the interaction energy evaluation. Water Res. 119, 33–46.
1341 https://doi.org/10.1016/j.watres.2017.04.041
1342 Liu, H., Huang, Q., Wang, Y., Xiao, C., 2017. PTFE conductive membrane for EVMD process and the
1343 application of electro-catalysis. Sep. Purif. Technol. https://doi.org/10.1016/j.seppur.2017.06.067
1344 Liu, L., Shen, F., Chen, X., Luo, J., Su, Y., Wu, H., Wan, Y., 2016. A novel plasma-induced surface

hydrophobization strategy for membrane distillation: Etching, dipping and grafting. J. Memb. Sci. 499, 544–554. https://doi.org/10.1016/j.memsci.2015.11.003

Liu, T., Li, X., Wang, D., Huang, Q., Liu, Z., Li, N., Xiao, C., 2016. Superhydrophobicity and regeneration of PVDF/SiO2 composite films. Appl. Surf. Sci. https://doi.org/10.1016/j.apsusc.2016.11.184

Lu, J., Yu, Y., Zhou, J., Song, L., Hu, X., Larbot, A., 2009. FAS grafted superhydrophobic ceramic membrane. Appl. Surf. Sci. 255, 9092–9099. https://doi.org/10.1016/j.apsusc.2009.06.112

Lu, K.-J., Zuo, J., Chung, T.-S., 2017. Novel PVDF membranes comprising n-butylamine functionalized graphene oxide for direct contact membrane distillation. J. Memb. Sci. 539, 34–42. https://doi.org/10.1016/j.memsci.2017.05.064

Lu, K.J., Zuo, J., Chung, T.S., 2016. Tri-bore PVDF hollow fibers with a super-hydrophobic coating for membrane distillation. J. Memb. Sci. 514, 165–175. https://doi.org/10.1016/j.memsci.2016.04.058

Lu, X., Peng, Y., Ge, L., Lin, R., Zhu, Z., Liu, S., 2016. Amphiphobic PVDF composite membranes for anti-fouling direct contact membrane distillation. J. Memb. Sci. 505, 61–69. https://doi.org/10.1016/j.memsci.2015.12.042

Lu, X., Peng, Y., Qiu, H., Liu, X., Ge, L., 2017. Anti-fouling membranes by manipulating surface wettability and their anti-fouling mechanism. Desalination 413, 127–135. https://doi.org/10.1016/j.desal.2017.02.022

Luo, A., Lior, N., 2017. Study of advancement to higher temperature membrane distillation. Desalination 419, 88–100. https://doi.org/10.1016/j.desal.2017.05.020

Ma, Z., Hong, Y., Ma, L., Su, M., 2009. Superhydrophobic Membranes with Ordered Arrays of Nanospiked Microchannels for Water Desalination. Langmuir 25, 5446–5450. https://doi.org/10.1021/la900494u

Majidi Salehi, S., Di Profio, G., Fontananova, E., Nicoletta, F.P., Curcio, E., De Filpo, G., 2016. Membrane distillation by novel hydrogel composite membranes. J. Memb. Sci. 504, 220–229. https://doi.org/10.1016/j.memsci.2015.12.062

Mansouri, J., Fane, A.G., 1999. Osmotic distillation of oily feeds. J. Memb. Sci. 153, 103–120. https://doi.org/10.1016/S0376-7388(98)00252-X

1371 Mapunda, E.C., Mamba, B.B., Msagati, T.A.M., 2017. Carbon nanotube embedded PVDF membranes:
1372 Effect of solvent composition on the structural morphology for membrane distillation. Phys. Chem.
1373 Earth, Parts A/B/C 1–8. https://doi.org/10.1016/j.pce.2017.01.003
1374 Martínez-Díez, L., Vázquez-González, M.., 1999. Temperature and concentration polarization in
1375 membrane distillation of aqueous salt solutions. J. Memb. Sci. 156, 265–273.
1376 https://doi.org/10.1016/S0376-7388(98)00349-4
1377 Matheswaran, M., Kwon, T., 2007. Factors affecting flux and water separation performance in air gap
1378 membrane distillation. J. Ind. Eng. Chem. 13, 965–970.
1379 McGaughey, A.L., Gustafson, R.D., Childress, A.E., 2017. Effect of long-term operation on membrane
1380 surface characteristics and performance in membrane distillation. J. Memb. Sci. 543, 143–150.
1381 https://doi.org/10.1016/j.memsci.2017.08.040
1382 McHale, G., Shirtcliffe, N.J., Newton, M.I., 2004. Super-hydrophobic and super-wetting surfaces:
1383 Analytical potential? Analyst 129, 284. https://doi.org/10.1039/b400567h
1384 Meng, S., Hsu, Y.C., Ye, Y., Chen, V., 2015a. Submerged membrane distillation for inland desalination
1385 applications. Desalination 361, 72–80. https://doi.org/10.1016/j.desal.2015.01.038
1386 Meng, S., Mansouri, J., Ye, Y., Chen, V., 2014a. Effect of templating agents on the properties and
1387 membrane distillation performance of TiO2-coated PVDF membranes. J. Memb. Sci. 450, 48–59.
1388 https://doi.org/10.1016/j.memsci.2013.08.036
1389 Meng, S., Ye, Y., Mansouri, J., Chen, V., 2015b. Crystallization behavior of salts during membrane
1390 distillation with hydrophobic and superhydrophobic capillary membranes. J. Memb. Sci. 473, 165–
1391 176. https://doi.org/10.1016/j.memsci.2014.09.024
1392 Meng, S., Ye, Y., Mansouri, J., Chen, V., 2014b. Fouling and crystallisation behaviour of superhydrophobic
1393 nano-composite PVDF membranes in direct contact membrane distillation. J. Memb. Sci. 463, 102–
1394 112. https://doi.org/10.1016/j.memsci.2014.03.027
1395 Mericq, J.P., Laborie, S., Cabassud, C., 2010. Vacuum membrane distillation of seawater reverse osmosis
1396 brines. Water Res. 44, 5260–5273. https://doi.org/10.1016/j.watres.2010.06.052

1397 Minier-Matar, J., Hussain, A., Janson, A., Benyahia, F., Adham, S., 2014. Field evaluation of membrane
1398 distillation technologies for desalination of highly saline brines. Desalination 351, 101–108.
1399 https://doi.org/10.1016/j.desal.2014.07.027
1400 Mohammadi, T., Akbarabadi, M., 2005. Separation of ethylene glycol solution by vacuum membrane
1401 distillation (VMD). Desalination 181, 35–41. https://doi.org/10.1016/j.desal.2005.01.012
1402 Mokhtar, N.M., Lau, W.J., Ismail, A.F., Kartohardjono, S., Lai, S.O., Teoh, H.C., 2016. The potential of
1403 direct contact membrane distillation for industrial textile wastewater treatment using PVDF-Cloisite
1404 15A nanocomposite membrane. Chem. Eng. Res. Des. 111, 284–293.
1405 https://doi.org/10.1016/j.cherd.2016.05.018
1406 Mokhtar, N.M., Lau, W.J., Ismail, A.F., Ng, B.C., 2014. Physicochemical study of polyvinylidene fluoride–
1407 Cloisite15A® composite membranes for membrane distillation application. RSC Adv. 4, 63367–
1408 63379. https://doi.org/10.1039/C4RA10289D
1409 Mokhtar, N.M., Lau, W.J., Ng, B.C., Ismail, A.F., Veerasamy, D., 2014. Preparation and characterization
1410 of PVDF membranes incorporated with different additives for dyeing solution treatment using
1411 membrane distillation. Desalin. Water Treat. 56, 1999–2012.
1412 https://doi.org/10.1080/19443994.2014.959063
1413 Moradi, R., Karimi-Sabet, J., Shariaty-Niassar, M., Koochaki, M.A., 2015. Preparation and characterization
1414 of polyvinylidene fluoride/graphene superhydrophobic fibrous films. Polymers (Basel). 7, 1444–
1415 1463. https://doi.org/10.3390/polym7081444
1416 Mostafa, M.G., Zhu, B., Cran, M., Dow, N., Milne, N., Desai, D., Duke, M., 2017. Membrane Distillation
1417 of Meat Industry Effluent with Hydrophilic Polyurethane Coated Polytetrafluoroethylene Membranes.
1418 Membranes (Basel). 7, 55. https://doi.org/10.3390/membranes7040055
1419 Naidu, G., Jeong, S., Choi, Y., Vigneswaran, S., 2017. Membrane distillation for wastewater reverse
1420 osmosis concentrate treatment with water reuse potential. J. Memb. Sci. 524, 565–575.
1421 https://doi.org/10.1016/j.memsci.2016.11.068
1422 Naidu, G., Jeong, S., Vigneswaran, S., 2014. Influence of feed/permeate velocity on scaling development

in a direct contact membrane distillation. Sep. Purif. Technol. 125, 291–300. https://doi.org/10.1016/j.seppur.2014.01.049

Naidu, G., Jeong, S., Vigneswaran, S., Hwang, T.-M., Choi, Y.-J., Kim, S.-H., 2015. A review on fouling of membrane distillation. Desalin. Water Treat. 3994, 1–25. https://doi.org/10.1080/19443994.2015.1040271

Nayar, K.G., Panchanathan, D., McKinley, G.H., Lienhard, J.H., 2014. Surface Tension of Seawater. J. Phys. Chem. Ref. Data 43, 43103. https://doi.org/10.1063/1.4899037

Nayar, K.G., Swaminathan, J., Warsinger, D.M., Lienhard, J.H., 2015. Performance Limits and Opportunities for Low Temperature Thermal Desalination, in: Proceedings of the 2015 India Water Week, 13-17 January. New Delhi.

Nayar, K.G., Swaminathan, J., Warsinger, D.M., McKinley, G.H., Lienhard, J.H., 2015. Effect of scale deposition on surface tension of seawater and membrane distillation. Proc. Int. Desalin. Assoc. World Congr. Desalin. Water Reuse, San Diego, CA, USA.

Nguyen, Q., Jeong, S., Lee, S., 2017. Characteristics of membrane foulants at different degrees of SWRO brine concentration by membrane distillation. Desalination 409, 7–20. https://doi.org/10.1016/j.desal.2017.01.007

Okiel, K., El-Aassar, A.H.M., Temraz, T., El-Etriby, S., Shawky, H.A., 2015. Performance assessment of synthesized CNT/polypropylene composite membrane distillation for oil field produced water desalination. Desalin. Water Treat. 1–13. https://doi.org/10.1080/19443994.2015.1044475

Onsekizoglu, P., 2012. Membrane Distillation: Principle, Advances, Limitations and Future Prospects in Food Industry, in: Distillation - Advances from Modeling to Applications. InTech. https://doi.org/10.5772/37625

Owens, D.K., Wendt, R.C., 1969. Estimation of the surface free energy of polymers. J. Appl. Polym. Sci. 13, 1741–1747. https://doi.org/10.1002/app.1969.070130815

Peña, L., de Zárate, J.M.O., Mengual, J.I., 1993. Steady states in membrane distillation: influence of membrane wetting. J. Chem. Soc., Faraday Trans. 89, 4333–4338.

https://doi.org/10.1039/FT9938904333

Peng, P., Fane, A.G., Li, X., 2005. Desalination by membrane distillation adopting a hydrophilic membrane. Desalination 173, 45–54. https://doi.org/10.1016/j.desal.2004.06.208

Peng, P., Ke, Q., Zhou, G., Tang, T., 2013. Fabrication of microcavity-array superhydrophobic surfaces using an improved template method. J. Colloid Interface Sci. 395, 326–328. https://doi.org/10.1016/j.jcis.2012.12.036

Peng, Y., Ge, J., Li, Z., Wang, S., 2015. Effects of anti-scaling and cleaning chemicals on membrane scale in direct contact membrane distillation process for RO brine concentrate. Sep. Purif. Technol. 154, 22–26. https://doi.org/10.1016/j.seppur.2015.09.007

Peng, Y., Ge, J., Wang, S., Li, Z., 2017. Occurrence of salt breakthrough and air-vapor pocket in a direct-contact membrane distillation. Desalination 402, 42–49. https://doi.org/10.1016/j.desal.2016.09.033

Politano, A., Argurio, P., Di Profio, G., Sanna, V., Cupolillo, A., Chakraborty, S., Arafat, H.A., Curcio, E., 2016. Photothermal Membrane Distillation for Seawater Desalination. Adv. Mater. 1–6. https://doi.org/10.1002/adma.201603504

Prince, J.A., Anbharasi, V., Shanmugasundaram, T.S., Singh, G., 2013. Preparation and characterization of novel triple layer hydrophilic–hydrophobic composite membrane for desalination using air gap membrane distillation. Sep. Purif. Technol. 118, 598–603. https://doi.org/10.1016/j.seppur.2013.08.006

Prince, J.A., Rana, D., Matsuura, T., Ayyanar, N., Shanmugasundaram, T.S., Singh, G., 2014a. Nanofiber based triple layer hydro-philic/-phobic membrane - a solution for pore wetting in membrane distillation. Sci. Rep. 4, 6949. https://doi.org/10.1038/srep06949

Prince, J.A., Rana, D., Singh, G., Matsuura, T., Jun Kai, T., Shanmugasundaram, T.S., 2014b. Effect of hydrophobic surface modifying macromolecules on differently produced PVDF membranes for direct contact membrane distillation. Chem. Eng. J. 242, 387–396. https://doi.org/10.1016/j.cej.2013.11.039

Prince, J.A., Singh, G., Rana, D., Matsuura, T., Anbharasi, V., Shanmugasundaram, T.S., 2012. Preparation and characterization of highly hydrophobic poly(vinylidene fluoride) - Clay nanocomposite nanofiber

membranes (PVDF-clay NNMs) for desalination using direct contact membrane distillation. J. Memb. Sci. 397–398, 80–86. https://doi.org/10.1016/j.memsci.2012.01.012

Purcell, W.R., 1950. Interpretation of Capillary Pressure Data. J. Pet. Technol. 2, 11–12. https://doi.org/10.2118/950369-G

Purwasasmita, M., Kurnia, D., Mandias, F.C., Khoiruddin, Wenten, I.G., 2015. Beer dealcoholization using non-porous membrane distillation. Food Bioprod. Process. 94, 180–186. https://doi.org/10.1016/j.fbp.2015.03.001

Qin, W., Zhang, J., Xie, Z., Ng, D., Ye, Y., Gray, S., Xie, M., 2016. Synergistic effect of combined colloidal and organic fouling in membrane distillation: measurements and mechanisms. Environ. Sci. Water Res. Technol. https://doi.org/10.1039/C6EW00156D

Qing, W., Shi, X., Deng, Y., Zhang, W., Wang, J., Tang, C.Y., 2017. Robust superhydrophobic-superoleophilic polytetrafluoroethylene nanofibrous membrane for oil/water separation. J. Memb. Sci. 540, 354–361. https://doi.org/10.1016/j.memsci.2017.06.060

Qtaishat, M.R., Banat, F., 2013. Desalination by solar powered membrane distillation systems. Desalination 308, 186–197. https://doi.org/10.1016/j.desal.2012.01.021

Qu, D., Wang, J., Wang, L., Hou, D., Luan, Z., Wang, B., 2009. Integration of accelerated precipitation softening with membrane distillation for high-recovery desalination of primary reverse osmosis concentrate. Sep. Purif. Technol. 67, 21–25. https://doi.org/10.1016/j.seppur.2009.02.021

Racz, G., Kerker, S., Schmitz, O., Schnabel, B., Kovacs, Z., Vatai, G., Ebrahimi, M., Czermak, P., 2015. Experimental determination of liquid entry pressure (LEP) in vacuum membrane distillation for oily wastewaters. Membr. Water Treat. 6, 237–249. https://doi.org/10.12989/mwt.2015.6.3.237

Rao, G., Hiibel, S.R., Childress, A.E., 2014. Simplified flux prediction in direct-contact membrane distillation using a membrane structural parameter. Desalination 351, 151–162. https://doi.org/10.1016/j.desal.2014.07.006

Ray, S.S., Chen, S.-S., Nguyen, N.C., Hsu, H.-T., Nguyen, H.T., Chang, C.-T., 2017. Poly(vinyl alcohol) incorporated with surfactant based electrospun nanofibrous layer onto polypropylene mat for

improved desalination by using membrane distillation. Desalination 414, 18–27. https://doi.org/10.1016/j.desal.2017.03.032

Razmjou, A., Arifin, E., Dong, G., Mansouri, J., Chen, V., 2012. Superhydrophobic modification of TiO2 nanocomposite PVDF membranes for applications in membrane distillation. J. Memb. Sci. 415–416, 850–863. https://doi.org/10.1016/j.memsci.2012.06.004

Rezaei, M., Samhaber, W., 2016a. Wetting study of Dual-Layer Hydrophilic / Hydrophobic Composite Membranes Coated with Nanoparticles for Membrane Distillation, in: DECHEMA.

Rezaei, M., Samhaber, W.M., 2017a. Impact of gas bubbling on wetting control in a submerged membrane distillation, in: 13th Minisymposium Der Verfahrenstechnik in Österreich.

Rezaei, M., Samhaber, W.M., 2017b. Impact of gas recharging on wetting control in membrane distillation for the concentration of highly saline brines, in: 3rd International Conference on Desalination Using Membrane Technology.

Rezaei, M., Samhaber, W.M., 2016b. Wetting Behaviour of Superhydrophobic Membranes Coated with Nanoparticles in Membrane Distillation. Chem. Eng. Trans. 47, 373–378. https://doi.org/10.3303/CET1647063

Rezaei, M., Samhaber, W.M., 2016c. Wetting control of Multiscale-Layer Membranes for Membrane Distillation, in: 12th Minisymposium Der Verfahrenstechnik. Graz, pp. 147–150. https://doi.org/10.3217/978-3-85125-456-3

Rezaei, M., Samhaber, W.M., 2015. Characterization of Macroporous Hydrophobic Membranes Used in Membrane Distillation Process, in: Filtech. p. 141.

Rezaei, M., Samhaber, W.M., 2014. Wetting phenomenon in membrane distillation processes, in: 10th Minisymposium Der Verfahrenstechnik. pp. 56–58.

Rezaei, M., Warsinger, D.M., Lienhard, J.H., Samhaber, W.M., 2017a. Wetting prevention in membrane distillation through superhydrophobicity and recharging an air layer on the membrane surface. J. Memb. Sci. 530, 42–52. https://doi.org/10.1016/j.memsci.2017.02.013

Rezaei, M., Warsinger, D.M., Lienhard, J.H., Samhaber, W.M., 2017b. Wetting prevention in membrane

distillation through superhydrophobicity and recharging an air layer on the membrane surface, Journal of Membrane Science. Elsevier. https://doi.org/10.1016/j.memsci.2017.02.013

Roy, Y., Warsinger, D.M., Lienhard, J.H., 2017. Effect of temperature on ion transport in nanofiltration membranes: Diffusion, convection and electromigration. Desalination 420, 241–257. https://doi.org/10.1016/j.desal.2017.07.020

Ruiz Salmón, I., Janssens, R., Luis, P., 2017. Mass and heat transfer study in osmotic membrane distillation-crystallization for CO2 valorization as sodium carbonate. Sep. Purif. Technol. 176, 173–183. https://doi.org/10.1016/j.seppur.2016.12.010

Saffarini, R.B., Mansoor, B., Thomas, R., Arafat, H.A., 2013. Effect of temperature-dependent microstructure evolution on pore wetting in PTFE membranes under membrane distillation conditions. J. Memb. Sci. 429, 282–294. https://doi.org/10.1016/j.memsci.2012.11.049

Sakai, K., Koyano, T., Muroi, T., Tamura, M., 1988. Effects of temperature and concentration polarization on water vapour permeability for blood in membrane distillation. Chem. Eng. J. 38, B33–B39. https://doi.org/10.1016/0300-9467(88)80081-9

Sanmartino, J.A., Khayet, M., García-Payo, M.C., El-Bakouri, H., Riaza, A., 2017. Treatment of reverse osmosis brine by direct contact membrane distillation: Chemical pretreatment approach. Desalination 420, 79–90. https://doi.org/10.1016/j.desal.2017.06.030

Sanmartino, J.A., Khayet, M., García-Payo, M.C., El Bakouri, H., Riaza, A., 2016. Desalination and concentration of saline aqueous solutions up to supersaturation by air gap membrane distillation and crystallization fouling. Desalination 393, 39–51. https://doi.org/10.1016/j.desal.2016.03.010

Sarti, G.C., Gostoli, C., Matulli, S., 1985. Low energy cost desalination processes using hydrophobic membranes. Desalination 56, 277–286. https://doi.org/10.1016/0011-9164(85)85031-1

Schneider, K., Hölz, W., Wollbeck, R., Ripperger, S., 1988a. Membranes and modules for transmembrane distillation. J. Memb. Sci. 39, 25–42. https://doi.org/10.1016/S0376-7388(00)80992-8

Schneider, K., Hölz, W., Wollbeck, R., Ripperger, S., 1988b. Membranes and modules for transmembrane distillation. J. Memb. Sci. 39, 25–42. https://doi.org/10.1016/S0376-7388(00)80992-8

1553 Schofield, R.W., Fane, A.G., Fell, C.J.D., 1990. Gas and vapour transport through microporous membranes.
1554 II. Membrane distillation. J. Memb. Sci. 53, 173–185.
1555 Schofield, R.W., Fane, A.G., Fell, C.J.D., Macoun, R., 1990. Factors affecting flux in membrane
1556 distillation. Desalination 77, 279–294. https://doi.org/10.1016/0011-9164(90)85030-E
1557 Servi, A.T., Kharraz, J., Klee, D., Notarangelo, K., Eyob, B., Guillen-Burrieza, E., Liu, A., Arafat, H.A.,
1558 Gleason, K.K., 2016. A systematic study of the impact of hydrophobicity on the wetting of MD
1559 membranes. J. Memb. Sci. 520, 850–859. https://doi.org/10.1016/j.memsci.2016.08.021
1560 Shaulsky, E., Nejati, S., Boo, C., Perreault, F., Osuji, C.O., Elimelech, M., 2017. Post-fabrication
1561 modification of electrospun nanofiber mats with polymer coating for membrane distillation
1562 applications. J. Memb. Sci. 530, 158–165. https://doi.org/10.1016/j.memsci.2017.02.025
1563 Shaw, D.J., 1992. Colloid & Surface Chemistry 315. https://doi.org/10.1007/s13398-014-0173-7.2
1564 Shin, Y., Cho, H., Choi, J., Sun Jang, Y., Choi, Y.-J., Sohn, J., Lee, S., Choi, J., 2016. Application of
1565 response surface methodology (RSM) in the optimization of dewetting conditions for flat sheet
1566 membrane distillation (MD) membranes. Desalin. Water Treat. 57, 10020–10030.
1567 https://doi.org/10.1080/19443994.2015.1038114
1568 Shin, Y., Choi, J., Lee, T., Sohn, J., Lee, S., 2015. Optimization of dewetting conditions for hollow fiber
1569 membranes in vacuum membrane distillation. Desalin. Water Treat. 1044266, 1–11.
1570 https://doi.org/10.1080/19443994.2015.1044266
1571 Shirazi, M.M.A., Kargari, A., Tabatabaei, M., 2015. Sweeping Gas Membrane Distillation (SGMD) as an
1572 Alternative for Integration of Bioethanol Processing: Study on a Commercial Membrane and
1573 Operating Parameters. Chem. Eng. Commun. 202, 457–466.
1574 https://doi.org/10.1080/00986445.2013.848805
1575 Shirazi, M.M.A., Kargari, A., Tabatabaei, M., 2014. Evaluation of commercial PTFE membranes in
1576 desalination by direct contact membrane distillation. Chem. Eng. Process. Process Intensif. 76, 16–
1577 25. https://doi.org/10.1016/j.cep.2013.11.010
1578 Silva, T.L.S., Morales-Torres, S., Figueiredo, J.L., Silva, A.M.T., 2015. Multi-walled carbon

nanotube/PVDF blended membranes with sponge- and finger-like pores for direct contact membrane distillation. Desalination 357, 233–245. https://doi.org/10.1016/j.desal.2014.11.025

Sirkar, K.K., Qin, Y., 2001. Novel membrane and device for direct contact membrane distillation based desalination process, DWPR Program Report No. 87.

Smolders, K., Franken, A.C.M., 1989. Terminology for Membrane Distillation. Desalination 72, 249–262. https://doi.org/10.1016/0011-9164(89)80010-4

Song, J., Huang, S., Hu, K., Lu, Y., Liu, X., Xu, W., 2013. Fabrication of Superoleophobic surfaces on Al Substrates. J. Mater. Chem. A 1. https://doi.org/10.1039/c3ta13807k

Song, L., Li, B., Sirkar, K.K., Gilron, J.L., 2007. Direct contact membrane distillation-based desalination: Novel membranes, devices, larger-scale studies, and a model. Ind. Eng. Chem. Res. 46, 2307–2323. https://doi.org/10.1021/ie0609968

Soni, V., Abildskov, J., Jonsson, G., Gani, R., 2008. Modeling and analysis of vacuum membrane distillation for the recovery of volatile aroma compounds from black currant juice. J. Memb. Sci. 320, 442–455. https://doi.org/10.1016/j.memsci.2008.04.025

Srisurichan, S., Jiraratananon, R., Fane, A.G., 2006. Mass transfer mechanisms and transport resistances in direct contact membrane distillation process. J. Memb. Sci. 277, 186–194. https://doi.org/10.1016/j.memsci.2005.10.028

Su, C., Chang, J., Tang, K., Gao, F., Li, Y., Cao, H., 2017. Novel Three-dimensional Superhydrophobic and Strength-enhanced Electrospun Membranes for Long-term Membrane Distillation. Sep. Purif. Technol. 178, 279–287. https://doi.org/10.1016/j.seppur.2017.01.050

Summers, E.K., Lienhard, J.H., 2013. Experimental study of thermal performance in air gap membrane distillation systems, including the direct solar heating of membranes. Desalination 330, 100–111. https://doi.org/10.1016/j.desal.2013.09.023

Swaminathan, J., Chung, H.W., Warsinger, D.M., AlMarzooqi, F.A., Arafat, H.A., Lienhard, J.H., 2016a. Energy efficiency of permeate gap and novel conductive gap membrane distillation. J. Memb. Sci. 502, 171–178. https://doi.org/10.1016/j.memsci.2015.12.017

Swaminathan, J., Chung, H.W., Warsinger, D.M., Lienhard, J.H., 2018. Membrane distillation at high salinity: evaluating critical system size and optimal membrane thickness. J. Memb. Sci. 211, 715–734. https://doi.org/10.1016/j.apenergy.2017.11.043

Swaminathan, J., Chung, H.W., Warsinger, D.M., Lienhard, J.H., 2018. Energy efficiency of membrane distillation up to high salinity: Evaluating critical system size and optimal membrane thickness. Appl. Energy 211, 715–734. https://doi.org/10.1016/j.apenergy.2017.11.043

Swaminathan, J., Chung, H.W., Warsinger, D.M., Lienhard, J.H., 2016b. Simple method for balancing direct contact membrane distillation. Desalination 383, 53–59. https://doi.org/10.1016/j.desal.2016.01.014

Swaminathan, J., Chung, H.W., Warsinger, D.M., Lienhard, J.H., 2016c. Membrane distillation model based on heat exchanger theory and configuration comparison. Appl. Energy 184, 491–505. https://doi.org/10.1016/j.apenergy.2016.09.090

Tan, Y.Z., Chew, J.W., Krantz, W.B., 2016. Effect of humic-acid fouling on membrane distillation. J. Memb. Sci. 504, 263–273. https://doi.org/10.1016/j.memsci.2015.12.051

Tan, Y.Z., Han, L., Chow, W.H., Fane, A.G., Chew, J.W., 2017. Influence of module orientation and geometry in the membrane distillation of oily seawater. Desalination 423, 111–123. https://doi.org/10.1016/j.desal.2017.09.019

Thomas, R., Guillen-Burrieza, E., Arafat, H.A., 2014. Pore structure control of PVDF membranes using a 2-stage coagulation bath phase inversion process for application in membrane distillation (MD). J. Memb. Sci. 452, 470–480. https://doi.org/10.1016/j.memsci.2013.11.036

Tian, M., Yin, Y., Yang, C., Zhao, B., Song, J., Liu, J., Li, X.-M., He, T., 2015. CF4 plasma modified highly interconnective porous polysulfone membranes for direct contact membrane distillation (DCMD). Desalination 369, 105–114. https://doi.org/10.1016/j.desal.2015.05.002

Tijing, L.D., Choi, J.S., Lee, S., Kim, S.H., Shon, H.K., 2014a. Recent progress of membrane distillation using electrospun nanofibrous membrane. J. Memb. Sci. 453, 435–462. https://doi.org/10.1016/j.memsci.2013.11.022

1631 Tijing, L.D., Woo, Y.C., Choi, J.-S., Lee, S., Kim, S.-H., Shon, H.K., 2015. Fouling and its control in
1632 membrane distillation—A review. J. Memb. Sci. 475, 215–244.
1633 https://doi.org/10.1016/j.memsci.2014.09.042
1634 Tijing, L.D., Woo, Y.C., Johir, M.A.H., Choi, J.S., Shon, H.K., 2014b. A novel dual-layer bicomponent
1635 electrospun nanofibrous membrane for desalination by direct contact membrane distillation. Chem.
1636 Eng. J. 256, 155–159. https://doi.org/10.1016/j.cej.2014.06.076
1637 Tijing, L.D., Woo, Y.C., Shim, W.G., He, T., Choi, J.S., Kim, S.H., Shon, H.K., 2016. Superhydrophobic
1638 nanofiber membrane containing carbon nanotubes for high-performance direct contact membrane
1639 distillation. J. Memb. Sci. 502, 158–170. https://doi.org/10.1016/j.memsci.2015.12.014
1640 Tomaszewska, M., 2000. Membrane distillation-examples of applications in technology and environmental
1641 protection. Polish J. Environ. Stud. 9, 27–36.
1642 Tong, D., Wang, X., Ali, M., Lan, C.Q., Wang, Y., Drioli, E., Wang, Z., Cui, Z., 2016. Preparation of
1643 Hyflon AD60/PVDF composite hollow fiber membranes for vacuum membrane distillation. Sep.
1644 Purif. Technol. 157, 1–8. https://doi.org/10.1016/j.seppur.2015.11.026
1645 Treybal, R.E., 1980. Mass-Transfer Operations, Mc Graw Hill International Book Company.
1646 Tuteja, A., Choi, W., Ma, M., Mabry, J.M., Mazzella, S.A., Rutledge, G.C., McKinley, G.H., Cohen, R.E.,
1647 2007. Designing Superoleophobic Surfaces. Science (80-.). 318, 1618–1622.
1648 https://doi.org/10.1126/science.1148326
1649 Tuteja, a, Choi, W., Mabry, J.M., McKinley, G.H., Cohen, R.E., 2008. Engineering superhydrophobic and
1650 superoleophobic surfaces. Tech. Proc. 2008 NSTI Nanotechnol. Conf. Trade Show, NSTI-Nanotech,
1651 Nanotechnol. 2008 1, 439–442.
1652 Walton, J., Lu, H., Turner, C., Solis, S., Hein, H., 2004. Solar and waste heat desalination by membrane
1653 distillation.
1654 Wang, F., Li, J., Zhu, H., Zhang, H., Tang, H., Chen, J., Guo, Y., 2014. Physical modification of
1655 polytetrafluoroethylene flat membrane by a simple heat setting process and membrane wetting
1656 remission in SGMD for desalination. Desalination 354, 143–152.

https://doi.org/10.1016/j.desal.2014.09.030

Wang, J., Qu, D., Tie, M., Ren, H., Peng, X., Luan, Z., 2008. Effect of coagulation pretreatment on membrane distillation process for desalination of recirculating cooling water. Sep. Purif. Technol. 64, 108–115. https://doi.org/10.1016/j.seppur.2008.07.022

Wang, J., Sun, X., Yuan, Y., Chen, H., Wang, H., Hou, D., 2016. A novel microwave assisted photo-catalytic membrane distillation process for treating the organic wastewater containing inorganic ions. J. Water Process Eng. 9, 1–8. https://doi.org/10.1016/j.jwpe.2015.11.004

Wang, K.Y., Chung, T.S., Gryta, M., 2008. Hydrophobic PVDF hollow fiber membranes with narrow pore size distribution and ultra-thin skin for the fresh water production through membrane distillation. Chem. Eng. Sci. 63, 2587–2594. https://doi.org/10.1016/j.ces.2008.02.020

Wang, P., Teoh, M.M., Chung, T.S., 2011. Morphological architecture of dual-layer hollow fiber for membrane distillation with higher desalination performance. Water Res. 45, 5489–5500. https://doi.org/10.1016/j.watres.2011.08.012

Wang, Y., Yu, Y., Hu, X., Feng, A., Jiang, F., Song, L., 2017. p -Phenylenediamine strengthened graphene oxide for the fabrication of superhydrophobic surface. Mater. Des. https://doi.org/10.1016/j.matdes.2017.04.033

Wang, Z., Elimelech, M., Lin, S., 2016a. Environmental Applications of Interfacial Materials with Special Wettability. Environ. Sci. Technol. 50, 2132–2150. https://doi.org/10.1021/acs.est.5b04351

Wang, Z., Hou, D., Lin, S., 2016b. Composite Membrane with Underwater-Oleophobic Surface for Anti-Oil-Fouling Membrane Distillation. Environ. Sci. Technol. 50, 3866–3874. https://doi.org/10.1021/acs.est.5b05976

Wang, Z., Lin, S., 2017. The impact of low-surface-energy functional groups on oil fouling resistance in membrane distillation. J. Memb. Sci. 527, 68–77. https://doi.org/10.1016/j.memsci.2016.12.063

Wang, Z., Tang, Y., Li, B., 2017. Excellent wetting resistance and anti-fouling performance of PVDF membrane modified with superhydrophobic papillae-like surfaces. J. Memb. Sci. 540, 401–410. https://doi.org/10.1016/j.memsci.2017.06.073

Warsinger, D., Swaminathan, J., Lienhard, J.H., 2014. Effect of Module Inclination Angle on Air Gap Membrane Distillation, in: Proceedings of the 15th International Heat Transfer Conference. Begellhouse, Connecticut, pp. 1–14. https://doi.org/10.1615/IHTC15.mtr.009351

Warsinger, D.E.M., 2015. Thermodynamic Design and Fouling of Membrane Distillation Systems. PhD thesis, Massachusetts Institute of Technology.

Warsinger, D.E.M., Swaminathan, J., Maswadeh, L.A., Lienhard, J.H., 2015. Superhydrophobic condenser surfaces for air gap membrane distillation. J. Memb. Sci. 492, 578–587. https://doi.org/10.1016/j.memsci.2015.05.067

Warsinger, D.M., Mistry, K.H., Nayar, K.G., Chung, H.W., Lienhard, J.H., 2015. Entropy Generation of Desalination Powered by Variable Temperature Waste Heat. Entropy 17, 7530–7566. https://doi.org/10.3390/e17117530

Warsinger, D.M., Servi, A., Connors, G., Gonzalez, J., Swaminathan, J., Chung, H.W., Arafat, H.A., Gleason, K.K., Lienhard, J.H., 2016. A novel air-cleaning method for membrane distillation, in: Proceedings of the AMTA Membrane Technology Conference & Exposition (MTC16). San Antonio, Texas.

Warsinger, D.M., Servi, A., Connors, G.B., Mavukkandy, M.O., Arafat, H.A., Gleason, K.K., Lienhard, J.H., 2017a. Reversing membrane wetting in membrane distillation: comparing dryout to backwashing with pressurized air. Environ. Sci. Water Res. Technol. 3, 930–939. https://doi.org/10.1039/C7EW00085E

Warsinger, D.M., Servi, A., Van Belleghem, S., Gonzalez, J., Swaminathan, J., Kharraz, J., Chung, H.W., Arafat, H.A., Gleason, K.K., Lienhard, J.H., 2016. Combining air recharging and membrane superhydrophobicity for fouling prevention in membrane distillation. J. Memb. Sci. 505, 241–252. https://doi.org/10.1016/j.memsci.2016.01.018

Warsinger, D.M., Swaminathan, J., Guillen-Burrieza, E., Arafat, H.A., Lienhard, J.H., 2015. Scaling and fouling in membrane distillation for desalination applications: A review. Desalination 356, 294–313. https://doi.org/10.1016/j.desal.2014.06.031

1709 Warsinger, D.M., Tow, E.W., Maswadeh, L.A., Connors, G., Swaminathan, J., Lienhard, J.H., 2018.
1710 Inorganic fouling mitigation by salinity cycling in batch reverse osmosis. Water Res.
1711 https://doi.org/10.1016/j.watres.2018.01.060
1712 Warsinger, D.M., Tow, E.W., Swaminathan, J., Lienhard, J.H., 2017b. Theoretical framework for
1713 predicting inorganic fouling in membrane distillation and experimental validation with calcium
1714 sulfate. J. Memb. Sci. 528, 381–390. https://doi.org/10.1016/j.memsci.2017.01.031
1715 Wei, C., Tang, Y., Zhang, G., Zhang, Q., Zhan, X., Chen, F., 2016. Facile fabrication of highly omniphobic
1716 and self-cleaning surfaces based on water mediated fluorinated nanosilica aggregation. RSC Adv. 6,
1717 74340–74348. https://doi.org/10.1039/C6RA13367C
1718 Wenzel, R.N., 1936. Resistance of Solid Surfaces To Wetting By Water. Ind. Eng. Chem. 28, 988–994.
1719 https://doi.org/10.1021/ie50320a024
1720 Woo, Y.C., Kim, Y., Shim, W.-G., Tijing, L.D., Yao, M., Nghiem, L.D., Choi, J.-S., Kim, S.-H., Shon,
1721 H.K., 2016a. Graphene/PVDF flat-sheet membrane for the treatment of RO brine from coal seam gas
1722 produced water by air gap membrane distillation. J. Memb. Sci. 513, 74–84.
1723 https://doi.org/10.1016/j.memsci.2016.04.014
1724 Woo, Y.C., Tijing, L.D., Park, M.J., Yao, M., Choi, J.S., Lee, S., Kim, S.H., An, K.J., Shon, H.K., 2015.
1725 Electrospun dual-layer nonwoven membrane for desalination by air gap membrane distillation.
1726 Desalination. https://doi.org/10.1016/j.desal.2015.09.009
1727 Woo, Y.C., Tijing, L.D., Shim, W.-G., Choi, J.-S., Kim, S.-H., He, T., Drioli, E., Shon, H.K., 2016b. Water
1728 desalination using graphene-enhanced electrospun nanofiber membrane via air gap membrane
1729 distillation. J. Memb. Sci. https://doi.org/10.1016/j.memsci.2016.07.049
1730 Wu, C., Li, Z., Zhang, J., Jia, Y., Gao, Q., Lu, X., 2015. Study on the heat and mass transfer in air-bubbling
1731 enhanced vacuum membrane distillation. Desalination 373, 16–26.
1732 https://doi.org/10.1016/j.desal.2015.07.001
1733 Wu, H., Shen, F., Wang, J., Luo, J., Liu, L., Khan, R., Wan, Y., 2016. Separation and concentration of ionic
1734 liquid aqueous solution by vacuum membrane distillation. J. Memb. Sci. 518, 216–228.

https://doi.org/10.1016/j.memsci.2016.07.017

Wu, Y., Kang, Y., Zhang, L., Qu, D., Cheng, X., Feng, L., 2017. Performance and fouling mechanism of direct contact membrane distillation (DCMD) treating fermentation wastewater with high organic concentrations. J. Environ. Sci. 1–9. https://doi.org/10.1016/j.jes.2017.01.015

Xiao, T., Wang, P., Yang, X., Cai, X., Lu, J., 2015. Fabrication and characterization of novel asymmetric polyvinylidene fluoride (PVDF) membranes by the nonsolvent thermally induced phase separation (NTIPS) method for membrane distillation applications. J. Memb. Sci. 489, 160–174. https://doi.org/10.1016/j.memsci.2015.03.081

Xiaoxing, S., Wenfang, Y., Qingfu, Z., 2011. Hydrophobic modification of PVDF 687, 658–661. https://doi.org/10.4028/www.scientific.net/MSF.687.658

Xu, J.B., Bartley, J.P., Johnson, R.A., 2005a. Application of Sodium Alginate- Carrageenan Coatings to PTFE Membranes for Protection Against Wet- Out by Surface- Active Agents. Sep. Sci. Technol. 40, 1067–1081. https://doi.org/10.1081/SS-200048167

Xu, J.B., Lange, S., Bartley, J.P., Johnson, R.A., 2004. Alginate-coated microporous PTFE membranes for use in the osmotic distillation of oily feeds. J. Memb. Sci. 240, 81–89. https://doi.org/10.1016/j.memsci.2004.04.016

Xu, J.B., Spittler, D.A., Bartley, J.P., Johnson, R.A., 2005b. Alginic acid-silica hydrogel coatings for the protection of osmotic distillation membranes against wet-out by surface-active agents. J. Memb. Sci. 260, 19–25. https://doi.org/10.1016/j.memsci.2005.03.017

Xu, W.T., Zhao, Z.P., Liu, M., Chen, K.C., 2015. Morphological and hydrophobic modifications of PVDF flat membrane with silane coupling agent grafting via plasma flow for VMD of ethanol-water mixture. J. Memb. Sci. 491, 110–120. https://doi.org/10.1016/j.memsci.2015.05.024

Xu, Z., Liu, Z., Song, P., Xiao, C., 2017. Fabrication of super-hydrophobic polypropylene hollow fiber membrane and its application in membrane distillation. Desalination 414, 10–17. https://doi.org/10.1016/j.desal.2017.03.029

Yan, H., Lu, X., Wu, C., Sun, X., Tang, W., 2017. Fabrication of a super-hydrophobic polyvinylidene

fluoride hollow fiber membrane using a particle coating process. J. Memb. Sci. 533, 130–140. https://doi.org/10.1016/j.memsci.2017.03.033

Yang, C., Li, X.M., Gilron, J., Kong, D. feng, Yin, Y., Oren, Y., Linder, C., He, T., 2014. CF4 plasma-modified superhydrophobic PVDF membranes for direct contact membrane distillation. J. Memb. Sci. 456, 155–161. https://doi.org/10.1016/j.memsci.2014.01.013

Yang, C., Tian, M., Xie, Y., Li, X.M., Zhao, B., He, T., Liu, J., 2015. Effective evaporation of CF4 plasma modified PVDF membranes in direct contact membrane distillation. J. Memb. Sci. 482, 25–32. https://doi.org/10.1016/j.memsci.2015.01.059

Yang, H.-C.C., Zhong, W., Hou, J., Chen, V., Xu, Z.-K.K., 2016. Janus hollow fiber membrane with a mussel-inspired coating on the lumen surface for direct contact membrane distillation. J. Memb. Sci. 523, 1–7. https://doi.org/10.1016/j.memsci.2016.09.044

Yang, W.F., Zhang, Z.Q., Gu, Z.Y., Shen, X.X., Zhang, Q.F., 2011. Research on the Superhydrophobic Modification of Polyvinylidene Fluoride Membrane. Adv. Mater. Res. 197–198, 514–517. https://doi.org/10.4028/www.scientific.net/AMR.197-198.514

Yang, X., Wang, R., Shi, L., Fane, A.G., Debowski, M., 2011. Performance improvement of PVDF hollow fiber-based membrane distillation process. J. Memb. Sci. 369, 437–447. https://doi.org/10.1016/j.memsci.2010.12.020

Yao, M., Woo, Y., Tijing, L., Cesarini, C., Shon, H., 2017. Improving Nanofiber Membrane Characteristics and Membrane Distillation Performance of Heat-Pressed Membranes via Annealing Post-Treatment. Appl. Sci. 7, 78. https://doi.org/10.3390/app7010078

Yin, X., Sun, C., Zhang, B., Song, Y., Wang, N., Zhu, L., Zhu, B., 2017. A facile approach to fabricate superhydrophobic coatings on porous surfaces using cross-linkable fluorinated emulsions. Chem. Eng. J. https://doi.org/10.1016/j.cej.2017.06.145

Young, T., 1807. A Course of Lectures on Natural Philosophy and the Mechanical Arts. Johnson.

Young, T., 1805. An Essay on the Cohesion of Fluids. Philos. Trans. R. Soc. London 95, 65–87. https://doi.org/10.1098/rstl.1805.0005

1787 Zakrzewska-Trznadel, G., Harasimowicz, M., Chmielewski, A.G., 1999. Concentration of radioactive
1788 components in liquid low-level radioactive waste by membrane distillation. J. Memb. Sci. 163, 257–
1789 264. https://doi.org/10.1016/S0376-7388(99)00171-4
1790 Zarebska, A., Amor, Á.C., Ciurkot, K., Karring, H., Thygesen, O., Andersen, T.P., Hägg, M.-B.,
1791 Christensen, K.V., Norddahl, B., 2015. Fouling mitigation in membrane distillation processes during
1792 ammonia stripping from pig manure. J. Memb. Sci. 484, 119–132.
1793 https://doi.org/10.1016/j.memsci.2015.03.010
1794 Zarebska, A., Nieto, D.R., Christensen, K. V., Norddahl, B., 2014. Ammonia recovery from agricultural
1795 wastes by membrane distillation: Fouling characterization and mechanism. Water Res. 56, 1–10.
1796 https://doi.org/10.1016/j.watres.2014.02.037
1797 Zhang, H., Lamb, R., Lewis, J., 2005. Engineering nanoscale roughness on hydrophobic surface -
1798 Preliminary assessment of fouling behaviour. Sci. Technol. Adv. Mater. 6, 236–239.
1799 https://doi.org/10.1016/j.stam.2005.03.003
1800 Zhang, J., Song, Z., Li, B., Wang, Q., Wang, S., 2013a. Fabrication and characterization of
1801 superhydrophobic poly (vinylidene fluoride) membrane for direct contact membrane distillation.
1802 Desalination 324, 1–9. https://doi.org/10.1016/j.desal.2013.05.018
1803 Zhang, J., Song, Z., Li, B., Wang, Q., Wang, S., 2013b. Fabrication and characterization of
1804 superhydrophobic poly (vinylidene fluoride) membrane for direct contact membrane distillation.
1805 Desalination 324, 1–9. https://doi.org/10.1016/j.desal.2013.05.018
1806 Zhang, P., Knötig, P., Gray, S., Duke, M., 2015. Scale reduction and cleaning techniques during direct
1807 contact membrane distillation of seawater reverse osmosis brine. Desalination 374, 20–30.
1808 https://doi.org/10.1016/j.desal.2015.07.005
1809 Zhang, W., Li, Y., Liu, J., Li, B., Wang, S., 2017. Fabrication of hierarchical poly (vinylidene fluoride)
1810 micro/nano-composite membrane with anti-fouling property for membrane distillation. J. Memb. Sci.
1811 https://doi.org/10.1016/j.memsci.2017.04.051
1812 Zhang, Y., Peng, Y., Ji, S., Li, Z., Chen, P., 2015. Review of thermal efficiency and heat recycling in

membrane distillation processes. Desalination 367, 223–239. https://doi.org/10.1016/j.desal.2015.04.013

Zhang, Y., Wang, X., Cui, Z., Drioli, E., Wang, Z., Zhao, S., 2017. Enhancing wetting resistance of poly(vinylidene fluoride) membranes for vacuum membrane distillation. Desalination 415, 58–66. https://doi.org/10.1016/j.desal.2017.04.011

Zhao, D., Zuo, J., Lu, K.-J., Chung, T.-S., 2017. Fluorographite modified PVDF membranes for seawater desalination via direct contact membrane distillation. Desalination 413, 119–126. https://doi.org/10.1016/j.desal.2017.03.012

Zhong, W., Hou, J., Yang, H.-C., Chen, V., 2017. Superhydrophobic membranes via facile bio-inspired mineralization for vacuum membrane distillation. J. Memb. Sci. https://doi.org/10.1016/j.memsci.2017.06.033

Zhu, J., Jiang, L., Matsuura, T., 2015. New insights into fabrication of hydrophobic/hydrophilic composite hollow fibers for direct contact membrane distillation. Chem. Eng. Sci. 137, 79–90. https://doi.org/10.1016/j.ces.2015.05.064

Zodrow, K.R., Bar-Zeev, E., Giannetto, M.J., Elimelech, M., 2014. Biofouling and Microbial Communities in Membrane Distillation and Reverse Osmosis. Environ. Sci. Technol. 48, 13155–13164. https://doi.org/10.1021/es503051t

Zuo, G., Wang, R., 2013. Novel membrane surface modification to enhance anti-oil fouling property for membrane distillation application. J. Memb. Sci. 447, 26–35. https://doi.org/10.1016/j.memsci.2013.06.053

Zuo, J., Chung, T.-S., 2016. Metal–Organic Framework-Functionalized Alumina Membranes for Vacuum Membrane Distillation. Water 8, 586. https://doi.org/10.3390/w8120586

Zuo, J., Chung, T.-S., O'Brien, G.S., Kosar, W., 2017. Hydrophobic/hydrophilic PVDF/Ultem® dual-layer hollow fiber membranes with enhanced mechanical properties for vacuum membrane distillation. J. Memb. Sci. 523, 103–110. https://doi.org/10.1016/j.memsci.2016.09.030

Zydney, A.L., 1995. Membrane handbook. AIChE J. 41, 2343–2344.

1839 https://doi.org/10.1002/aic.690411024

1840

Highlights

- This review offers an extensive literature survey on the wetting phenomenon in MD.
- Describes wetting fundamentals, equations, parameters, and measurement techniques
- Analyzes wetting conditions, effects, prevention, and reversal techniques
- This review lays the groundwork for future technological advances in MD.

Graphical Abstract